JAERI-Research
95-060

# TIME BEHAVIOUR OF HEAT DIFFUSIVITY DURING L-H-L TRANSITIONS IN JT-60U

September 1995

Sergei V. NEUDATCHIN*, Tomonori TAKIZUKA, Hiroshi SHIRAI, Nobuaki ISEI
Yutaka KAMADA, Yoshihiko KOIDE, Masayasu SATO and Masafumi AZUMI

日本原子力研究所
Japan Atomic Energy Research Institute

本レポートは，日本原子力研究所が不定期に公刊している研究報告書です。
入手の問合わせは，日本原子力研究所技術情報部情報資料課（〒319-11 茨城県那珂郡東海村）あて，お申し越しください。なお，このほかに財団法人原子力弘済会資料センター（〒319-11 茨城県那珂郡東海村日本原子力研究所内）で複写による実費頒布をおこなっております。

This report is issued irregularly.
Inquiries about availability of the reports should be addressed to Information Division, Department of Technical Information, Japan Atomic Energy Research Institute, Tokai-mura, Naka-gun, Ibaraki-ken 319-11, Japan.



編集兼発行　日本原子力研究所
印　　刷　㈱原子力資料サービス

# Time Behaviour of Heat Diffusivity during L-H-L Transitions in JT－60U

Sergei V. NEUDATCHIN*, Tomonori TAKIZUKA, Hiroshi SHIRAI, Nobuaki ISEI
Yutaka KAMADA, Yoshihiko KOIDE, Masayasu SATO and Masafumi AZUMI

Department of Fusion Plasma Research
Naka Fusion Research Establishment
Japan Atomic Energy Research Institute
Naka-machi, Naka-gun, Ibaraki-ken

(Received August 18, 1995)

The L-H-L transitions have been analyzed mainly for high field pulses ($B_t \approx 4T$) in JT－60U. The simultaneous response of electron temperature $T_e$ has been clearly observed during L-H-L transitions over the wide plasma region. This $T_e$ evolution is described as the result of the fast jump of electron heat diffusivity, $\delta\chi_e$, over the wide plasma region. Values of $\delta\chi_e$ were obtained as $0.5\,m^2/s < |\delta\chi_e| < 1\,m^2/s$. They usually increase with radius. The simultaneous response of ion temperature Ti was also observed similarly to the $T_e$ response. The jump of ion heat diffusivity, $\delta\chi_i$, is similar to $\delta\chi_e$ and usually increases with radius as the same as $\delta\chi_e$. In a low field pulse($B_t \approx 2.5T$), $|\delta\chi_i|$ is as large as $2\,m^2/s$. Values of $\delta\chi$ are consistent with the change of the energy confinement time during transitions. The dependence of $\delta\chi_i$ is negative on $B_t$ or $I_p$ like $1/B_t$ or $1/I_p$, while the $B_t$ or $I_p$ dependence of $\delta\chi_e$ is weak. These $I_p$ dependencies agree qualitatively with the result of the power balance analysis of JT－60U L-mode plasmas.

Keywords: Tokamak, JT－60U, Transport, H-mode, L-H Transition, H-L Transition, Heat Diffusivity, Electron Temperature, Ion Temperature

---

* Russian Research Center "Kurchatov Institute"

# JT－60U中のL-H-L遷移時における熱拡散係数の時間的挙動

日本原子力研究所那珂研究所炉心プラズマ研究部
Sergei V. NEUDATCHIN*・滝塚　知典・白井　浩・伊世井宣明
鎌田　裕・小出　芳彦・佐藤　正泰・安積　正史

（1995年8月18日受理）

JT－60Uの主に高磁場放電（$B_t = 4T$）におけるL-H-L遷移について解析を行った。L-H-L遷移時に，プラズマの広い領域に亙り同時的な電子温度$T_e$の応答が観測された。この$T_e$の時間変化は，プラズマの広い領域に亙る電子熱拡散係数の速い跳び$\delta\chi_e$に因るものである。この$\delta\chi_e$の絶対値，$0.5m^2/s < |\delta\chi_e| < 1m^2/s$，を求めた。これは通常，半径方向に大きくなっている。イオン温度の同時的な応答が$T_e$の応答と同様であることも観測した。イオン熱拡散係数の跳び$\delta\chi_i$もまた，$\delta\chi_e$と同様な値であり，半径方向に増大する。弱磁場放電（$B_t = 2.5T$）においては，$|\delta\chi_i|$は$2m^2/s$まで大きくなっている。これらの$\delta\chi$の値は，遷移前後のエネルギー閉じ込め時間の変化と矛盾しない。イオン熱拡散係数の跳び$\delta\chi_i$は$B_t$または$I_p$に対し$1/B_t$または$1/I_p$のような反対的依存性をしている。一方，$\delta\chi_e$は$B_t$または$I_p$に弱くしか依存しない。これらの$I_p$依存性は，JT-60Uのしモードプラズマのパワーバランス解析の結果と定性的に一致している。

那珂研究所：〒311-01　茨城県那珂郡那珂町向山801-1
＊クルチャトフ研究所

Contents



# 目　　次

## 1. Introduction

An understanding of the time evolution of local transport coefficients during a transition between various confinement regimes is important to clarify the physical mechanism responsible for the anomalous transport observed in tokamak plasmas.

In relation to L-H-L transitions, soft terminations and strong ELMs on JET, the time evolutions of electron temperature $T_e$, ion temperature $T_i$, electron heat diffusivity $\chi_e$, and ion heat diffusivity $\chi_i$ have been analyzed and reported previously [1-4]. The simultaneous $T_e$ response (with few millisecond uncertainty) was clearly seen during L-H-L transitions in the plasma region, $0.2 < r/a < 1$ (r is the volume-averaged minor radius of a magnetic surface and a is the volume-averaged minor radius of the separatrix). To describe this event, we apply a simple heat diffusion equation with the change in $\chi_e$ after the transition. It was shown that $\chi_e$ changes across almost all plasma volume on a millisecond time scale (more than a hundred times faster than the energy confinement time $\tau_E$). It can be considered that the anomalous L-mode transport is switched on and off on a millisecond time scale during transitions. Values of $\chi_e$ jump, $\delta\chi_e$, were easily obtained from experimental data. Note that these values can be calculated without knowing values of power balance diffusivity $\chi^{PB}$ before and after a transition. Interestingly, the profile of $T_e$ gradient was almost unchanged in a limited space-time region by these transitions, but value of $T_e$ was changed. The behaviours of $T_i$ and toroidal rotation velocity $V_t$ were similar to $T_e$, and values of $\delta\chi_i$ and $\delta\chi_{mom}$ were obtained also. It was not obvious up to today whether these diffusivity jumps are the peculiar feature of JET or not.

The possible explanation for the jump of $\chi$ is that a part of the anomalous transport is controlled by "noise pumping" created by strong periphery turbulence [5]. The density fluctuation level and the correlation width measured by correlation reflectometry technique decrease simultaneously with $\chi_e$ variation at the L-H-L transitions on JET [3, 4]. The similar picture of the density turbulence behaviour at a transition was observed on JT-60U [6].

Let us remind that in the "traditional picture" the L-H or H-L transition occurs near the plasma surface, and the confinement improvement in plasma interior then evolves on a time scale of the order of $\tau_E$ [7].

Results of JET above mentioned [1-4] were severely criticized by Burrel [8]. The criticism seems based on the DIII-D results where the "traditional picture" was seen. This criticism seems also based on the result of the heat pulse propagation (HPP) study: The author of Ref. [8] might mix the fast $T_e$ response during L-H-L transitions on JET with the short term (within one millisecond usually) non-diffusive spreading of the $T_e$ perturbation during a sawtooth crash on TFTR[9] and JET [2, 10]. He suggested in Ref. [8] to use "inward heat pinch model" to describe JET

data. The unrealistic value of convective electron heat velocity (order of 100 m/s) is obviously necessary for the propagation of the $T_e$ response over one meter within few milliseconds on JET. We believe, therefore, that the "inward heat pinch model" cannot be applied to describe the L-H-L transitions on JET.

In order to answer above questions, we investigate in the present paper the time evolution of $\chi_e$ and $\chi_i$ during L-H-L transitions on JT-60U. The behaviour of $T_e$ is measured by ECE grating polychromator [11] and that of $T_i$ is measured by charge-exchange recombination spectroscopy [12]. It is well-known that the confinement behaviour in various stages of the discharges on JT-60U is complicatedly varied with plasma parameters. There are no clear first L-H transitions in many JT-60U high field pulses [6, 13]. The formation of the internal transport barrier occurs before or independently from the edge barrier formation [14]. Regarding any types of confinement modes, we restrict the analyses here for the cases of L-H-L transitions after the improved confinement with high H-factor (ratio of $\tau_E$ to $\tau_E^{ITER89P}$) is well developed. In the next section, jumps of $\chi$ during transitions are analyzed mainly for high field pulses. Section 3 is devoted to discussion on the results. Conclusion is summarized in section 4.

## 2. Analyses of $\delta\chi$ during transitions

In this section, we analyze the jumps of $\chi$, $\delta\chi$, during L-H-L transitions on JT-60U mainly for high field pulses, i.e., the toroidal magnetic field at the plasma center $B_t$ is about 4 T. Typical shape parameters are the major radius $R \approx 3.2$ m, the volume-averaged minor radius $a \approx 1.05$ m, the ellipticity $\kappa \approx 1.6$, the triangularity $\delta < 0.1$, and the plasma volume $V \approx 70$ m$^3$. We study the behaviours of $\chi_e$ in sub-section 2.1 and of $\chi_i$ in sub-section 2.2. The behaviour of $\chi_i$ for a low field pulse ($B_t = 2.5$ T) is also analyzed for comparison in sub-section 2.3.

### 2.1 Electron heat diffusivity

At first, we study the response of $\chi_e$ during an H-L transition. The waveforms of a hot ion H mode pulse 16130 with $I_p/B_t = 3$ MA/4.2 T [6] are shown in Fig. 1. In the figure, the plasma current $I_p$, the line integrated electron density $n_eL$ (length L is about 2.5 m), the stored energy measured by diamagnetic loop W, the injected neutral beam power $P_{NB}$, and the H$\alpha$ intensity from the divertor region H$\alpha_{div}$ are shown. The time evolution of electron temperature profile, $T_e(r, t)$, was observed with JT-60U multi-channel ECE grating polychromator [11]. The signals were calibrated from Fourier transform spectrometer system [15]. Figures 2 and 3 show $T_e(\rho, t)$ in the low field side and $T_e(\rho, t)$ in the high field side, respectively, where $\rho = r/a$ is the normalized minor radius. The time evolutions of $T_e(\rho)$ in both sides are basically the same with each other. In ECE signals, spikes induced by ELMs (Edge

data. The unrealistic value of convective electron heat velocity (order of 100 m/s) is obviously necessary for the propagation of the $T_e$ response over one meter within few milliseconds on JET. We believe, therefore, that the "inward heat pinch model" cannot be applied to describe the L-H-L transitions on JET.

In order to answer above questions, we investigate in the present paper the time evolution of $\chi_e$ and $\chi_i$ during L-H-L transitions on JT-60U. The behaviour of $T_e$ is measured by ECE grating polychromator [11] and that of $T_i$ is measured by charge-exchange recombination spectroscopy [12]. It is well-known that the confinement behaviour in various stages of the discharges on JT-60U is complicatedly varied with plasma parameters. There are no clear first L-H transitions in many JT-60U high field pulses [6, 13]. The formation of the internal transport barrier occurs before or independently from the edge barrier formation [14]. Regarding any types of confinement modes, we restrict the analyses here for the cases of L-H-L transitions after the improved confinement with high H-factor (ratio of $\tau_E$ to $\tau_E^{ITER89P}$) is well developed. In the next section, jumps of $\chi$ during transitions are analyzed mainly for high field pulses. Section 3 is devoted to discussion on the results. Conclusion is summarized in section 4.

## 2. Analyses of $\delta\chi$ during transitions

In this section, we analyze the jumps of $\chi$, $\delta\chi$, during L-H-L transitions on JT-60U mainly for high field pulses, i.e., the toroidal magnetic field at the plasma center $B_t$ is about 4 T. Typical shape parameters are the major radius $R \approx 3.2$ m, the volume-averaged minor radius $a \approx 1.05$ m, the ellipticity $\kappa \approx 1.6$, the triangularity $\delta < 0.1$, and the plasma volume $V \approx 70$ m$^3$. We study the behaviours of $\chi_e$ in sub-section 2.1 and of $\chi_i$ in sub-section 2.2. The behaviour of $\chi_i$ for a low field pulse ($B_t = 2.5$ T) is also analyzed for comparison in sub-section 2.3.

### 2.1 Electron heat diffusivity

At first, we study the response of $\chi_e$ during an H-L transition. The waveforms of a hot ion H mode pulse 16130 with $I_p/B_t = 3$ MA/4.2 T [6] are shown in Fig. 1. In the figure, the plasma current $I_p$, the line integrated electron density $n_eL$ (length L is about 2.5 m), the stored energy measured by diamagnetic loop W, the injected neutral beam power $P_{NB}$, and the H$\alpha$ intensity from the divertor region H$\alpha_{div}$ are shown. The time evolution of electron temperature profile, $T_e(r, t)$, was observed with JT-60U multi-channel ECE grating polychromator [11]. The signals were calibrated from Fourier transform spectrometer system [15]. Figures 2 and 3 show $T_e(\rho, t)$ in the low field side and $T_e(\rho, t)$ in the high field side, respectively, where $\rho = r/a$ is the normalized minor radius. The time evolutions of $T_e(\rho)$ in both sides are basically the same with each other. In ECE signals, spikes induced by ELMs (Edge

Localized Modes) are superimposed. Since we pay attention to only the monotonous evolution of the ECE signals, we excluded large spikes of ECE signals from the figures in this paper.

It is clearly seen that the growth of the stored energy W is interrupted by a series of ELMs. The decay of all ECE signals is clearly seen during the short L-mode phase for an approximately 30 ms time interval pointed as A-B. After the time B, the improved confinement recovers in the ELM-free H-mode phase. The L-mode again starts from the time C. The value of $\tau_E \equiv W/(P_{abs} - dW/dt)$ in the L-mode decreases by factor of two from that in the H-mode; $\tau_E$ during B-C is about 400 ms ($H \approx 1.6$), and $\tau_E$ after C is about 200 ms ($H \approx 1.1$), where we assume $P_{abs} = 0.8\ P_{NB}$ by considering the shine through loss and the prompt ripple loss. The beginning of the decay of ECE signals over the region $0.1 < r/a < 0.8$ and the jump of $H_\alpha$ occur simultaneously (about 10 ms uncertainties). Moreover we see an interesting and unusual feature of the transition C. The $T_e$ decay for $0.2 < r/a < 0.4$ is sharper and earlier than that around $r/a = 0.8$. This rules out the possibility of the HPP from the periphery. Probably it is connected with complicated structure of transition in this particular case; the jump of $\chi_e$ for $0.2 < r/a < 0.4$ occurs initially and $\chi_e$ increases slowly near $r/a = 0.8$. The propagation speed is estimated to be of order of 10 m/s.

Typical pictures for L-H and H-L transitions are seen in a so-called "steady-state high $\beta_p$ ELMy H mode" pulse 21282 with 2.3 MA/4.2 T [16]. This plasma has a small volume, $V \approx 50\ m^3$, compared with other plasmas, $V \approx 70\ m^3$, analyzed in this paper. The waveforms of this discharge are shown in Fig. 4. The end of "steady-state phase" is around 7.5 s. Two L modes (A-B and C-D in Fig. 5) with transitions back to H-mode are clearly observed on the $H_\alpha$ and W signals. Values of $\tau_E$ after A and C are about 180 ms ($H \approx 1.5$) and $\tau_E \approx 450$ ms ($H \approx 2.3$) after B and D. In Fig. 5, one can see that the time behaviours of $T_e(\rho=0.66)$ and $T_e(\rho=0.5)$ are similar to that of W within 10 ms uncertainty. For the central region, $r/a = 0.35$ and 0.21, however, the time delay of $T_e$ response is clearly seen as was observed in JET [1-4]. This result shows that HPP may play important role near the center or that the improvement and degradation of transport may propagate from the mid region to the center with the propagation speed of about 10 m/s. As for the outer region $r/a > 0.7$, since there was no ECE channel available, we cannot analyze in detail the difference between plasmas of the 16130 pulse and the 21282 pulse.

It is natural for us to explain the sudden change in $T_e$ at a transition caused by sudden variation of the electron heat flux. As described in Refs. [1-4] we apply a simple heat diffusion equation with the change in $\chi_e$ across almost all plasma volume after the transition. The value of $\chi_e$ jump, $\delta\chi_e$, can be estimated from a simple formula,

$$\delta\chi_e(r) \cong \frac{3}{2}\frac{1}{n_e \nabla T_e(r) A(r)} \int_0^{V(r)} n_e \frac{\partial \delta T_e}{\partial t}\, dV , \qquad (1)$$

where A(r) and V(r) are the surface area and the enclosed volume at the radius r, respectively. Heat sources, such as neutral beam heating power, Joule heating power, and energy transfer between electrons and ions, are considered here to be unchanged or to be changed only negligibly. The reliability of the formula (1) was checked with both interpretative and predictive transport calculations in Refs. [2-4].

In the 16130 pulse, the value of $\delta\chi_e$ after the H-L transition (C in Fig. 2) is about 0.75 $m^2/s$ at $r/a \approx 0.35$ and 0.6 $m^2/s$ at $r/a \approx 0.64$. After the L-H transition (D in Fig. 5) in the pulse 21282, the value of $\delta\chi_e$ is about -0.85 $m^2/s$ at $r/a \approx 0.58$.

## 2.2 Ion heat diffusivity

Next we analyze jumps of ion heat diffusivity, $\delta\chi_i$, as well as $\delta\chi_e$. The evolution of plasma parameters in a 3.5 MA/4.1 T hot ion H-mode pulse 17058 are shown in Fig. 6. The growth of W is interrupted by a clear H-L transition at the time A and the improved confinement does not recover later. The value of $\tau_E$ before A is about 380 ms ($H \approx 1.5$) and $\tau_E \approx 190$ ms ($H \approx 1.0$) after A. The evolution of the $T_e$ profile is shown in Fig. 7. A sawtooth crash occurs about 50 ms after the transition. The $T_e$ in the region $0.43 < r/a < 0.83$ varies simultaneously after the transition A, while in the central region, $r/a < 0.36$, the $T_e$ is changed slowly as the same as for 16130 pulse. Values of $\delta\chi_e$ are about 0.65 $m^2/s$ and 0.85 $m^2/s$ at $r/a \approx 0.61$ and 0.71, respectively.

Figure 8 shows the evolution of $T_i$ profile, $T_i(\rho, t)$, which behaves similarly to the $T_e(\rho, t)$. We can see more clearly the correlation between $V_t(\rho, t)$ and $T_e(\rho, t)$ in Fig. 9. The toroidal rotation is in counter direction for the H-mode phase, and decreases its speed after the H-L transition. Note that the time resolution of $T_i$ and $V_t$ measurement was about 17 ms. Assuming that the decrease of $T_i(\rho)$ starts together with $T_e(\rho)$ after the transition, we obtain the value of $\delta\chi_i$ from Eq. (1) as $\delta\chi_i \approx 0.55$ $m^2/s$ at $r/a \approx 0.56$.

In the similar discharges with similar transitions, almost the same values of $\delta\chi$ are observed. Figure 10 shows the waveforms of a 3.5 MA/4.2T pulse 17160, where plasma parameters are similar to those in the pulse 17158. The $T_i(\rho, t)$ is also shown in the figure. Values of $\delta\chi_i$ is about 0.58 $m^2/s$ at $r/a \approx 0.63$ and $\delta\chi_e \approx 0.77$ $m^2/s$ at $r/a \approx 0.73$.

The L-H and H-L transitions in a low-Ip pulse 17038 (2 MA/4.2 T) are shown in Figs. 11, 12 and 13. During short ELM-free H-mode phases (A-B and C-D in Figs. 12 and 13) values of $\tau_E$ are about 330 ms ($H \approx 1.8$), while during high-$T_i$ L-

mode phases (before A, B-C, and after D) $\tau_E \approx 190$ ms ($H \approx 1.3$). The simultaneous response of $T_e$ and $T_i$ over the wide region, $0.3 < r/a < 0.8$, is clearly seen in Figs. 12 and 13. The value of $\delta\chi_e$ is about -0.65 $m^2/s$ at $r/a \approx 0.63$, of which absolute value is almost the same as those at $r/a \approx 0.6$ for higher-Ip pulses above analyzed. On the other hand, values of $\delta\chi_i$ after an L-H transition are about -0.64 $m^2/s$ and -0.93 $m^2/s$ at $r/a \approx 0.55$ and 0.63, respectively. These values are almost the same as or a little higher than those for high-Ip pulses.

### 2.3 Transitions in a low field pulse

For the low field pulse in JT-60U, we found yet only one example with clear L-H-L transitions in a1.5 MA/2.5 T pulse 17298 [6]. The evolution of some plasma parameters and the $T_i(\rho, t)$ is presented in Fig. 14. During the L-mode phase, A-B in the figure, the value of $\tau_E$ is about 130 ms ($H \approx 1.3$), and $\tau_E \approx 250$ ms ($H \approx 1.8$) during the H-mode phase, B-C. Similarly to JET result [3, 4], high values of $\delta\chi_i$ are obtained compared with those in high field pulses; $\delta\chi_i \approx$ -0.85, -1.3 and -2.0 $m^2/s$ at $r/a \approx 0.44$, 0.52 and 0.60, respectively. The polychromator data, $T_e(\rho, t)$, are not available to use for low field pulses, $B_t < 3.5$ T, because the grating filter is optimized for $B_t \approx 4$ T.

## 3. Discussion

We have analyzed L-H-L transitions in JT-60U and evaluated values of $\delta\chi$. Plasma parameters and values of $\delta\chi_e$ and $\delta\chi_i$ are summarized in Tables 1 - 6.

We examine whether these values of $\delta\chi$ are consistent with the change of $\tau_E$ during transitions. Though the value of $\tau_E$ was calculated not from the thermal stored energy but from the total stored energy including fast ion component, the following approximate relation is used for the comparison between $|\delta\chi|$ and the change of $\tau_E$; $\tau_E \approx a^2/4\chi_{\rho\approx0.6}$ and $|\delta\chi_{\rho\approx0.6}| \approx (a^2/4)\{\tau_E(L)^{-1} - \tau_E(H)^{-1}\}$. Here we consider cases of $\delta\chi_e \approx \delta\chi_i$ and the smooth radial variation of $\delta\chi$. Typical values of $\tau_E(L)$ and $\tau_E(H)$ in plasmas of $a \approx 1.05$ m are about 0.2 s and 0.4 s, respectively, and the value of $|\delta\chi_{\rho\approx0.6}|$ is about 0.6 $m^2/s$. These values roughly satisfy the above relation. This result supports the validity of the present model in which $\chi$ jumps simultaneously over the wide plasma region during a transition.

Next we discuss about the characteristics of $\delta\chi$ comparing our results and JET data [1-4]. The simultaneous response of $T_e$ over wide plasma region with the $H_\alpha$ signal were observed in both JT-60U and JET. Values of $\delta\chi_e$ in JT-60U and JET are similar; $0.5\ m^2/s < |\delta\chi_e| < 1\ m^2/s$ in the plasma mid region, $r/a \sim 0.5$. The expression of $\delta\chi_e \sim q^2\,\nabla(n_eT_e)/(n_eB_t)$ in JET [3, 4, 17] is applied to the JT-60U data, but the poor agreement is found with the error of about factor 2.

As for the ratio of $\delta\chi_i$ to $\delta\chi_e$, it is almost unity for JT60U with $B_t \approx 4$ T, while it

mode phases (before A, B-C, and after D) $\tau_E \approx 190$ ms ($H \approx 1.3$). The simultaneous response of $T_e$ and $T_i$ over the wide region, $0.3 < r/a < 0.8$, is clearly seen in Figs. 12 and 13. The value of $\delta\chi_e$ is about -0.65 $m^2/s$ at $r/a \approx 0.63$, of which absolute value is almost the same as those at $r/a \approx 0.6$ for higher-Ip pulses above analyzed. On the other hand, values of $\delta\chi_i$ after an L-H transition are about -0.64 $m^2/s$ and -0.93 $m^2/s$ at $r/a \approx 0.55$ and 0.63, respectively. These values are almost the same as or a little higher than those for high-Ip pulses.

### 2.3 Transitions in a low field pulse

For the low field pulse in JT-60U, we found yet only one example with clear L-H-L transitions in a1.5 MA/2.5 T pulse 17298 [6]. The evolution of some plasma parameters and the $T_i(\rho, t)$ is presented in Fig. 14. During the L-mode phase, A-B in the figure, the value of $\tau_E$ is about 130 ms ($H \approx 1.3$), and $\tau_E \approx 250$ ms ($H \approx 1.8$) during the H-mode phase, B-C. Similarly to JET result [3, 4], high values of $\delta\chi_i$ are obtained compared with those in high field pulses; $\delta\chi_i \approx$ -0.85, -1.3 and -2.0 $m^2/s$ at $r/a \approx 0.44$, 0.52 and 0.60, respectively. The polychromator data, $T_e(\rho, t)$, are not available to use for low field pulses, $B_t < 3.5$ T, because the grating filter is optimized for $B_t \approx 4$ T.

## 3. Discussion

We have analyzed L-H-L transitions in JT-60U and evaluated values of $\delta\chi$. Plasma parameters and values of $\delta\chi_e$ and $\delta\chi_i$ are summarized in Tables 1 - 6.

We examine whether these values of $\delta\chi$ are consistent with the change of $\tau_E$ during transitions. Though the value of $\tau_E$ was calculated not from the thermal stored energy but from the total stored energy including fast ion component, the following approximate relation is used for the comparison between $|\delta\chi|$ and the change of $\tau_E$; $\tau_E \approx a^2/4\chi_{\rho\approx0.6}$ and $|\delta\chi_{\rho\approx0.6}| \approx (a^2/4)\{\tau_E(L)^{-1} - \tau_E(H)^{-1}\}$. Here we consider cases of $\delta\chi_e \approx \delta\chi_i$ and the smooth radial variation of $\delta\chi$. Typical values of $\tau_E(L)$ and $\tau_E(H)$ in plasmas of $a \approx 1.05$ m are about 0.2 s and 0.4 s, respectively, and the value of $|\delta\chi_{\rho\approx0.6}|$ is about 0.6 $m^2/s$. These values roughly satisfy the above relation. This result supports the validity of the present model in which $\chi$ jumps simultaneously over the wide plasma region during a transition.

Next we discuss about the characteristics of $\delta\chi$ comparing our results and JET data [1-4]. The simultaneous response of $T_e$ over wide plasma region with the $H_\alpha$ signal were observed in both JT-60U and JET. Values of $\delta\chi_e$ in JT-60U and JET are similar; $0.5\ m^2/s < |\delta\chi_e| < 1\ m^2/s$ in the plasma mid region, $r/a \sim 0.5$. The expression of $\delta\chi_e \sim q^2\,\nabla(n_eT_e)/(n_eB_t)$ in JET [3, 4, 17] is applied to the JT-60U data, but the poor agreement is found with the error of about factor 2.

As for the ratio of $\delta\chi_i$ to $\delta\chi_e$, it is almost unity for JT60U with $B_t \approx 4$ T, while it

was about 3 for a low field pulse (3 MA / 1.9 T) on JET [3,4]. For a low field pulse (1.5 MA / 2.5 T) on JT-60U, only $\delta\chi_i$ values were evaluated (see sub-section 2.3). These values are about three times larger than those for high field pulses on JT-60U, but similar to those of JET data. If we combine JT-60U data and JET data together, we suppose that the dependence of $\delta\chi_i$ is negative on $B_t$ like $1/B_t$, while the dependence of $\delta\chi_e$ is weak on $B_t$. Therefore the ratio $\delta\chi_i / \delta\chi_e$ may have a negative dependence on $B_t$. The tendency of the negative dependence on $I_p$ is also seen for $\delta\chi_i$. The increase of $\chi_i^{PB}$ with decrease of $I_p$ in JT-60U L-mode plasmas was found from the power balance analysis [18]. The weak $I_p$ dependence of $\chi_e^{PB}$ was also reported in Ref. [18]. These dependencies on $I_p$ are in qualitative agreement with each other.

## 4. Conclusion

We have analyzed L-H-L transitions mainly for high field pulses in JT-60U. The simultaneous $T_e$ response (with uncertainty of 10 ms) has been clearly observed during L-H-L transitions over $0.2 < r/a < 0.9$ in JT-60U plasmas similarly in JET [1-4]. Plasma parameters are $B_t \approx 4$ T, 2 MA $< I_p <$ 3.5 MA, $3.2 < q_{eff} < 5.9$, $V \approx 70$ m$^3$ (one pulse with $V \approx 50$ m$^3$), $1.9 \times 10^{19}$ m$^{-3} < n_e < 3.4 \times 10^{19}$ m$^{-3}$ , 20 MW $< P_{NB} <$ 30 MW, and 4 MJ $< W <$ 8 MJ during time intervals studied. This evolution of $T_e(\rho, t)$ is difficult to be explained as the result of the heat pulse propagation (HPP) from the periphery, but is reasonable to be described as the result of the fast $\chi_e$ jump (reduction at L-H transitions and increment at H-L transitions) over $0.2 < r/a < 0.9$. The fast variation of $\chi$ (at least 20-40 times less than $\tau_E$) inside almost all plasma volume is a new finding of the L-H-L transitions in JT-60U. The $T_e$ response in the central region ($r/a \sim 0.3$) often delays compared with that in the outer region ($r/a \sim 0.5$), and the role of HPP could be important similarly to JET results [1-4]. Values of $\delta\chi_e$ were obtained for $0.5 < r/a < 0.7$, 3.5 keV$< T_e <$ 5.5 keV, and 6 keV/m $< \nabla T_e <$ 8 keV/m, whose absolute values were 0.6 m$^2$/s $< |\delta\chi_e| <$ 0.9 m$^2$/s. They usually increase with radius.

We have also evaluated $\delta\chi_i$ during L-H-L transitions mainly for high field pulses in JT-60U. The transitions in a low field pulse (1.5 MA / 2.5 T) was analyzed for comparison. The simultaneous $T_i$ response (with uncertainty of 20 ms) were also observed similarly to the $T_e$ response. Values of $\delta\chi_i$ were obtained for $0.4 < r/a < 0.7$, 4 keV$< T_i <$ 12 keV, and 10 keV/m $< \nabla T_i <$ 17 keV/m. Their absolute values usually increase with radius as the same as $\delta\chi_e$. In high $I_p$ pulses ($I_p >$ 3 MA / $B_t$ = 4.2 T), values of $|\delta\chi_i| \approx 0.5$ m$^2$/s are almost the same as or a little smaller than those of $|\delta\chi_e|$, while in a low $I_p$ pulse (2 MA / 4.2 T), values of 0.6 m$^2$/s $< |\delta\chi_i| <$ 1 m$^2$/s are almost the same or a little larger than $|\delta\chi_e|$. In a low field pulse (1.5 MA / 2.5 T), values of $|\delta\chi_i|$ are rather large as 2 m$^2$/s at $r/a \approx 0.60$.

was about 3 for a low field pulse (3 MA / 1.9 T) on JET [3,4]. For a low field pulse (1.5 MA / 2.5 T) on JT-60U, only $\delta\chi_i$ values were evaluated (see sub-section 2.3). These values are about three times larger than those for high field pulses on JT-60U, but similar to those of JET data. If we combine JT-60U data and JET data together, we suppose that the dependence of $\delta\chi_i$ is negative on $B_t$ like $1/B_t$, while the dependence of $\delta\chi_e$ is weak on $B_t$. Therefore the ratio $\delta\chi_i / \delta\chi_e$ may have a negative dependence on $B_t$. The tendency of the negative dependence on $I_p$ is also seen for $\delta\chi_i$. The increase of $\chi_i^{PB}$ with decrease of $I_p$ in JT-60U L-mode plasmas was found from the power balance analysis [18]. The weak $I_p$ dependence of $\chi_e^{PB}$ was also reported in Ref. [18]. These dependencies on $I_p$ are in qualitative agreement with each other.

## 4. Conclusion

We have analyzed L-H-L transitions mainly for high field pulses in JT-60U. The simultaneous $T_e$ response (with uncertainty of 10 ms) has been clearly observed during L-H-L transitions over $0.2 < r/a < 0.9$ in JT-60U plasmas similarly in JET [1-4]. Plasma parameters are $B_t \approx 4$ T, 2 MA $< I_p <$ 3.5 MA, $3.2 < q_{eff} < 5.9$, $V \approx 70$ m$^3$ (one pulse with $V \approx 50$ m$^3$), $1.9 \times 10^{19}$ m$^{-3} < n_e < 3.4 \times 10^{19}$ m$^{-3}$ , 20 MW $< P_{NB} <$ 30 MW, and 4 MJ $< W <$ 8 MJ during time intervals studied. This evolution of $T_e(\rho, t)$ is difficult to be explained as the result of the heat pulse propagation (HPP) from the periphery, but is reasonable to be described as the result of the fast $\chi_e$ jump (reduction at L-H transitions and increment at H-L transitions) over $0.2 < r/a < 0.9$. The fast variation of $\chi$ (at least 20-40 times less than $\tau_E$) inside almost all plasma volume is a new finding of the L-H-L transitions in JT-60U. The $T_e$ response in the central region ($r/a \sim 0.3$) often delays compared with that in the outer region ($r/a \sim 0.5$), and the role of HPP could be important similarly to JET results [1-4]. Values of $\delta\chi_e$ were obtained for $0.5 < r/a < 0.7$, 3.5 keV$< T_e <$ 5.5 keV, and 6 keV/m $< \nabla T_e <$ 8 keV/m, whose absolute values were 0.6 m$^2$/s $< |\delta\chi_e| <$ 0.9 m$^2$/s. They usually increase with radius.

We have also evaluated $\delta\chi_i$ during L-H-L transitions mainly for high field pulses in JT-60U. The transitions in a low field pulse (1.5 MA / 2.5 T) was analyzed for comparison. The simultaneous $T_i$ response (with uncertainty of 20 ms) were also observed similarly to the $T_e$ response. Values of $\delta\chi_i$ were obtained for $0.4 < r/a < 0.7$, 4 keV$< T_i <$ 12 keV, and 10 keV/m $< \nabla T_i <$ 17 keV/m. Their absolute values usually increase with radius as the same as $\delta\chi_e$. In high $I_p$ pulses ($I_p >$ 3 MA / $B_t$ = 4.2 T), values of $|\delta\chi_i| \approx 0.5$ m$^2$/s are almost the same as or a little smaller than those of $|\delta\chi_e|$, while in a low $I_p$ pulse (2 MA / 4.2 T), values of 0.6 m$^2$/s $< |\delta\chi_i| <$ 1 m$^2$/s are almost the same or a little larger than $|\delta\chi_e|$. In a low field pulse (1.5 MA / 2.5 T), values of $|\delta\chi_i|$ are rather large as 2 m$^2$/s at $r/a \approx 0.60$.

Values of $\delta\chi$ are consistent with the change of $\tau_E$ during transitions. The dependence of $\delta\chi_i$ is negative on $B_t$ or $I_p$ like $1/B_t$ or $1/I_p$, while the $B_t$.or $I_p$ dependence of $\delta\chi_e$ is weak. These $I_p$ dependencies agree qualitatively with the result of power balance analysis for JT-60U L-mode plasmas [18].

We have no $B_t$ scan data nor other parameter scan data to study dependencies of $\delta\chi$ on $B_t$, $I_p$, $n_e$, $T$ , $\nabla T$ etc. It is necessary to investigate $\delta\chi$ further with the ECE measurement at low field and the high time resolution $T_i$ measurement in new JT-60U experiments.

## Acknowledgments

One of the authors (S.V.N.) wish to acknowledge Drs. J.G. Cordey and D.G. Muir of JET for fruitful discussions and encouragement. This work was performed when SVN was visiting to JAERI under the JAERI foreign researcher inviting program. He is grateful to the JAERI for hospitality and financial support.

Values of $\delta\chi$ are consistent with the change of $\tau_E$ during transitions. The dependence of $\delta\chi_i$ is negative on $B_t$ or $I_p$ like $1/B_t$ or $1/I_p$, while the $B_t$.or $I_p$ dependence of $\delta\chi_e$ is weak. These $I_p$ dependencies agree qualitatively with the result of power balance analysis for JT-60U L-mode plasmas [18].

We have no $B_t$ scan data nor other parameter scan data to study dependencies of $\delta\chi$ on $B_t$, $I_p$, $n_e$, $T$ , $\nabla T$ etc. It is necessary to investigate $\delta\chi$ further with the ECE measurement at low field and the high time resolution $T_i$ measurement in new JT-60U experiments.

## Acknowledgments

One of the authors (S.V.N.) wish to acknowledge Drs. J.G. Cordey and D.G. Muir of JET for fruitful discussions and encouragement. This work was performed when SVN was visiting to JAERI under the JAERI foreign researcher inviting program. He is grateful to the JAERI for hospitality and financial support.

## References


[1] S. V. Neudatchin, J. G. Cordey, D. G. Muir, "The Time Behaviour of the Electron Conductivity during L-H and H-L Transitions in JET", JET-P(93) 58 (1993).

[2] S. V. Neudatchin, J. G. Cordey, D. G. Muir, in Contr. Fusion and Plasma Phys. (Proc. Eur. Conf., Lisboa, 1993) **Vol. 17c, part 1** (EPS, 1993) 83.

[3] J. G. Cordey, D. G. Muir, S. V. Neudatchin, V. V. Parail, S. Ali-Arshad, D. V. Bartlett, D. J. Campbell, A. E. Costley, A. L. Colton, A. W. Edwards, L. Porte, A. C. C. Sips, E. P. Springmann, P. M. Stubberfield, G. Vayakis, W. G. von Hellermann, A. Taroni and K. Thomsen, Plasma Phys. and Contr. Fusion **36 Suppl.** (1994) A267.

[4] J. G. Cordey, D. G. Muir, S. V. Neudatchin, V. V. Parail, E. Springmann and A. Taroni, Nucl. Fusion **35** (1995) 101.

[5] B. B. Kadomtsev, Plasma Phys. and Contr. Fusion **34** (1992) 1931.

[6] T. Fukuda, M. Kikuchi, Y. Koide, M. Sato, Y. Neyatani and M. Azumi, Plasma Phys. and Contr. Fusion **36 Suppl.** (1994) A87.

[7] R. J. Groebner, Phys. Fluids B **5** (1993) 2343.

[8] K. H. Burrell, Plasma Phys. and Contr. Fusion **36 Suppl.** (1994) A291.

[9] E. D. Fredrickson, A. C. Janos, K. M. McGuire, S. D. Scott, G. Taylor and Z. Chang, Nucl. Fusion **33** (1993) 1759.

[10] S. V. Neudatchin and D.G. Muir, "The Study of Electron Heat Transport in JET by Analysing the Decay of Temperature Perturbations Induced by Sawteeth", JET-P(93) 27 (1993).

[11] S. Ishida, A. Nagashima, M. Sato, N. Isei and T. Matoba, Rev. Sci. Instrum. **61** (1990) 2864.

[12] Y. Koide, S. Ishida, A. Sakasai, H. Shirai, T. Hirayama, H. Kubo, T. Sugie and A. Funahashi, Nucl. Fusion **33** (1993) 251.

[13] M. Mori, the JT-60 Team and the JFT-2M Team, Plasma Phys. and Contr. Fusion **36 Suppl.** (1994) A39.

[14] Y. Koide, S. Ishida, M. Kikuchi, M. Mori, S. Tsuji, T. Nishitani, Y. Kawano, T. Hatae, T. Fujita, T. Ozeki, H. Shirai, Y. Kamada, R. Yoshino, H. Ninomiya, M. Azumi and the JT-60 Team, 15th Int. Conf. on Plasma Phys. and Contr. Nucl. Fusion Research, Seville, 1994, IAEA-CN-60/A-2-I-3.

[15] M. Sato, N. Isei, S. Ishida, T. Aoyagi and T. Hirayama, "Fourier Transform Spectrometer System in JT-60U", in "Review of JT-60U Experimental Results from March to October, 1991", JAERI-M 92-073 (1992) pp.342-343.

[16] Y. Kamada, K. Ushigusa, Y. Neyatani, O. Naito, T. Ozeki, Y. Kawano, R. Yoshino, H. Kubo, T. Fujita, S. Ishida, M. Sato, Y. Koide, S. Takeji, S. Sakurai, K. Tsuchiya, J. Manickam, M. Matsuoka, M. Kikuchi, M. Mori, H. Ninomiya, M. Azumi and the JT-60 Team, 15th Int. Conf. on Plasma Phys. and Contr. Nucl. Fusion Research, Seville, 1994, IAEA-CN-60/A-5-I-5.

[17] V. V. Parail, B. Balet, P. Bak, J. G. Cordey, N. Deliyanakis, M. Erba, R. Giannella, D. G. Muir, M. F. F. Nave, L. Porte, E. M. Springmann, A. Taroni, K. Thomsen and G. Vayakis, 15th Int. Conf. on Plasma Phys. and Contr. Nucl. Fusion Research, Seville, 1994, IAEA-CN-60/A-2-II-3.

[18] H. Shirai, T. Takizuka and M. Azumi, Proc. of International School of Plasma Physics, Varenna, Italy, 1993, (SIF, Bologna, 1993) p.33.

Table 1 Plasma parameters and $\delta\chi$ values for 16130 pulse

| shot No | $I_p$ (MA) | $B_t$ (T) | $q_{eff}$ | V ($m^3$) | W (MJ) |
|---|---|---|---|---|---|
| 16130 | 3.0 | 4.2 | 3.78 | 68 | 5.9 |

| t (s) | type | ρ | $\delta\chi$ ($m^2/s$) | T (keV) | $\nabla T$ (keV/m) | $n_e$ ($10^{19}m^{-3}$) |
|---|---|---|---|---|---|---|
| 7.17 | H-L | 0.64 | $\delta\chi_e = +0.60$ | $T_e = 5.4$ | $\nabla T_e = 7.5$ | $n_e(U2) = 3.4$ |

Table 2 Plasma parameters and $\delta\chi$ values for 21282 pulse

| shot No | $I_p$ (MA) | $B_t$ (T) | $q_{eff}$ | V ($m^3$) | W (MJ) |
|---|---|---|---|---|---|
| 21282 | 2.3 | 4.2 | 4.08 | 51 | 5.7 |

| t (s) | type | ρ | $\delta\chi$ ($m^2/s$) | T (keV) | $\nabla T$ (keV/m) | $n_e$ ($10^{19}m^{-3}$) |
|---|---|---|---|---|---|---|
| 7.92 | L-H | 0.58 | $\delta\chi_e = -0.85$ | $T_e = 5.4$ | $\nabla T_e = 7.5$ | $n_e(U2) = 2.5$ |

Table 3 Plasma parameters and $\delta\chi$ values for 17058 pulse

| shot No | $I_p$ (MA) | $B_t$ (T) | $q_{eff}$ | V ($m^3$) | W (MJ) |
|---|---|---|---|---|---|
| 17058 | 3.5 | 4.2 | 3.37 | 70 | 6.8 |

| t (s) | type | ρ | $\delta\chi$ ($m^2/s$) | T (keV) | $\nabla T$ (keV/m) | $n_e$ ($10^{19}m^{-3}$) |
|---|---|---|---|---|---|---|
| 8.38 | H-L | 0.56 | $\delta\chi_i = +0.55$ | $T_i = 11.5$ | $\nabla T_i = 16.5$ | $n_e(U2) = 3.3$ |
| | | 0.61 | $\delta\chi_e = +0.65$ | $T_e = 5.0$ | $\nabla T_e = 6.5$ | |
| | | 0.71 | $\delta\chi_e = +0.85$ | $T_e = 4.5$ | $\nabla T_e = 6.0$ | |

Table 4 Plasma parameters and $\delta\chi$ values for 17060 pulse

| shot No | $I_p$ (MA) | $B_t$ (T) | $q_{eff}$ | V ($m^3$) | W (MJ) |
|---|---|---|---|---|---|
| 17060 | 3.5 | 4.2 | 3.25 | 68 | 7.6 |

| t (s) | type | ρ | $\delta\chi$ ($m^2/s$) | T (keV) | $\nabla T$ (keV/m) | $n_e$ ($10^{19}m^{-3}$) |
|---|---|---|---|---|---|---|
| 8.49 | H-L | 0.63 | $\delta\chi_i = +0.58$ | $T_i = 9.0$ | $\nabla T_i = 16.0$ | $n_e(U2) = 3.3$ |
| | | 0.73 | $\delta\chi_e = +0.77$ | $T_e = 4.5$ | $\nabla T_e = 6.5$ | |

Table 5 Plasma parameters and $\delta\chi$ values for 17038 pulse

| shot No | $I_p$ (MA) | $B_t$ (T) | $q_{eff}$ | V ($m^3$) | W (MJ) |
|---|---|---|---|---|---|
| 17038 | 2.0 | 4.2 | 5.85 | 68 | 4.5 |

| t (s) | type | ρ | $\delta\chi$ ($m^2/s$) | T (keV) | $\nabla T$ (keV/m) | $n_e$ ($10^{19}m^{-3}$) |
|---|---|---|---|---|---|---|
| 7.15 | L-H | 0.55 | $\delta\chi_i = -0.64$ | $T_i = 7.0$ | $\nabla T_i = 12.0$ | $n_e(U2) = 1.9$ |
| | | 0.63 | $\delta\chi_i = -0.93$ | $T_i = 6.0$ | $\nabla T_i = 13.0$ | |
| | | 0.63 | $\delta\chi_e = -0.65$ | $T_e = 3.5$ | $\nabla T_e = 6.0$ | |

Table 6 Plasma parameters and $\delta\chi$ values for 17298 pulse

| shot No | $I_p$ (MA) | $B_t$ (T) | $q_{eff}$ | V ($m^3$) | W (MJ) |
|---|---|---|---|---|---|
| 17298 | 1.5 | 2.5 | 4.46 | 70 | 2.8 |

| t (s) | type | ρ | $\delta\chi$ ($m^2/s$) | T (keV) | $\nabla T$ (keV/m) | $n_e$ ($10^{19}m^{-3}$) |
|---|---|---|---|---|---|---|
| 5.71 | L-H | 0.44 | $\delta\chi_i = -0.85$ | $T_i = 5.7$ | $\nabla T_i = 10.0$ | $n_e(U2) = 1.3$ |
| | | 0.52 | $\delta\chi_i = -1.3$ | $T_i = 4.8$ | $\nabla T_i = 10.0$ | |
| | | 0.60 | $\delta\chi_i = -2.0$ | $T_i = 3.9$ | $\nabla T_i = 8.0$ | |

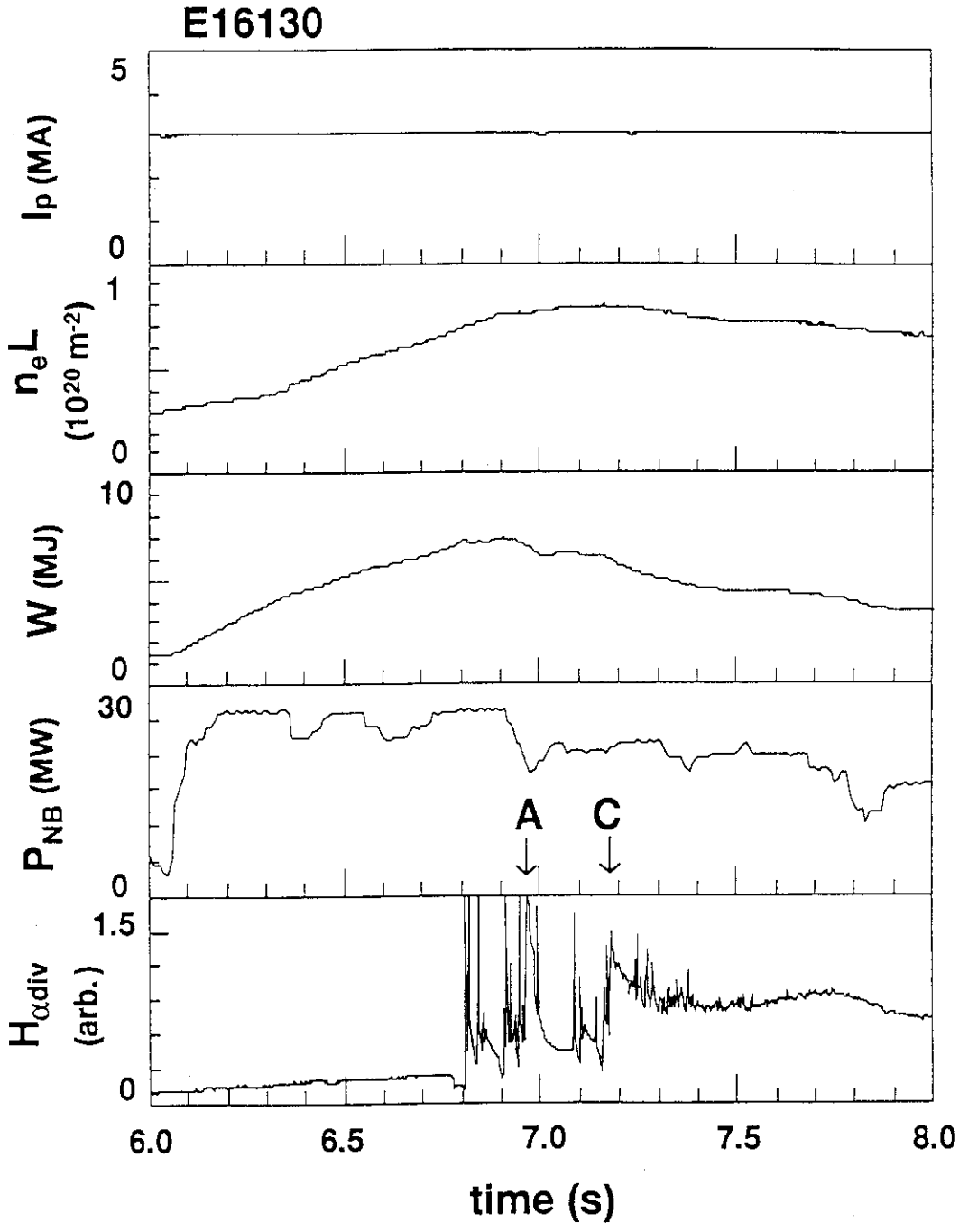


Fig. 1 Waveforms of a hot ion H mode pulse 16130 (3 MA/4.2 T). Plasma current $I_p$ (MA), line integrated electron density $n_eL$ ($10^{20}m^{-2}$), stored energy measured by diamagnetic loop W (MJ), injected neutral beam power $P_{NB}$ (MW), and $H\alpha$ intensity from the divertor region $H\alpha_{div}$ (arbitrary unit) are shown. H-L transitions of interest are pointed by arrows A and C.

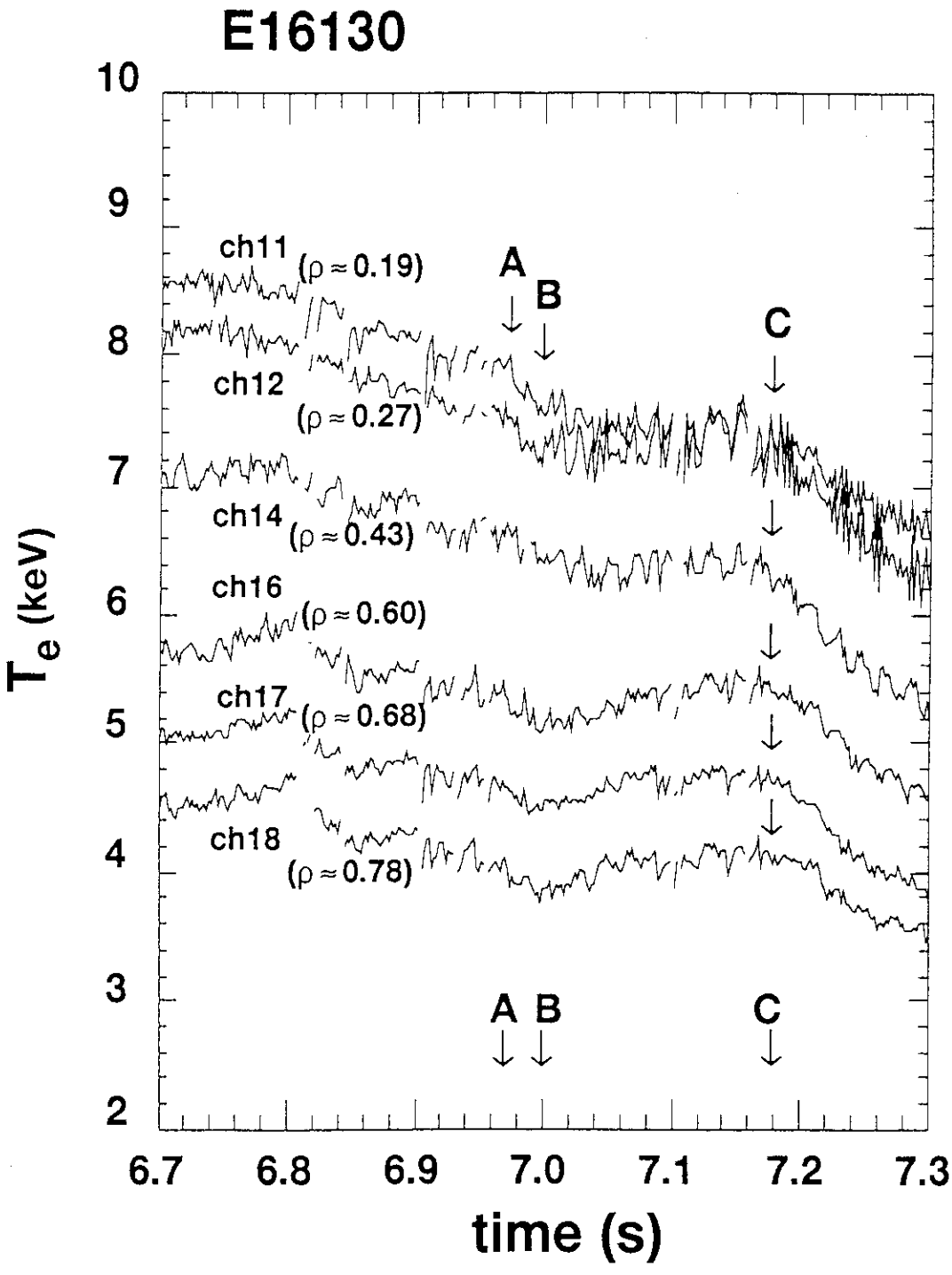


Fig. 2 Time evolution of electron temperature profile, $T_e(\rho, t)$, for 16130 pulse. Channel number of ECE grating polychromator and radial position ($\rho = r/a$) in the low field side are shown. Time of interest is pointed by an arrow. Simultaneous response of $T_e$ during transitions is seen over the wide plasma region.

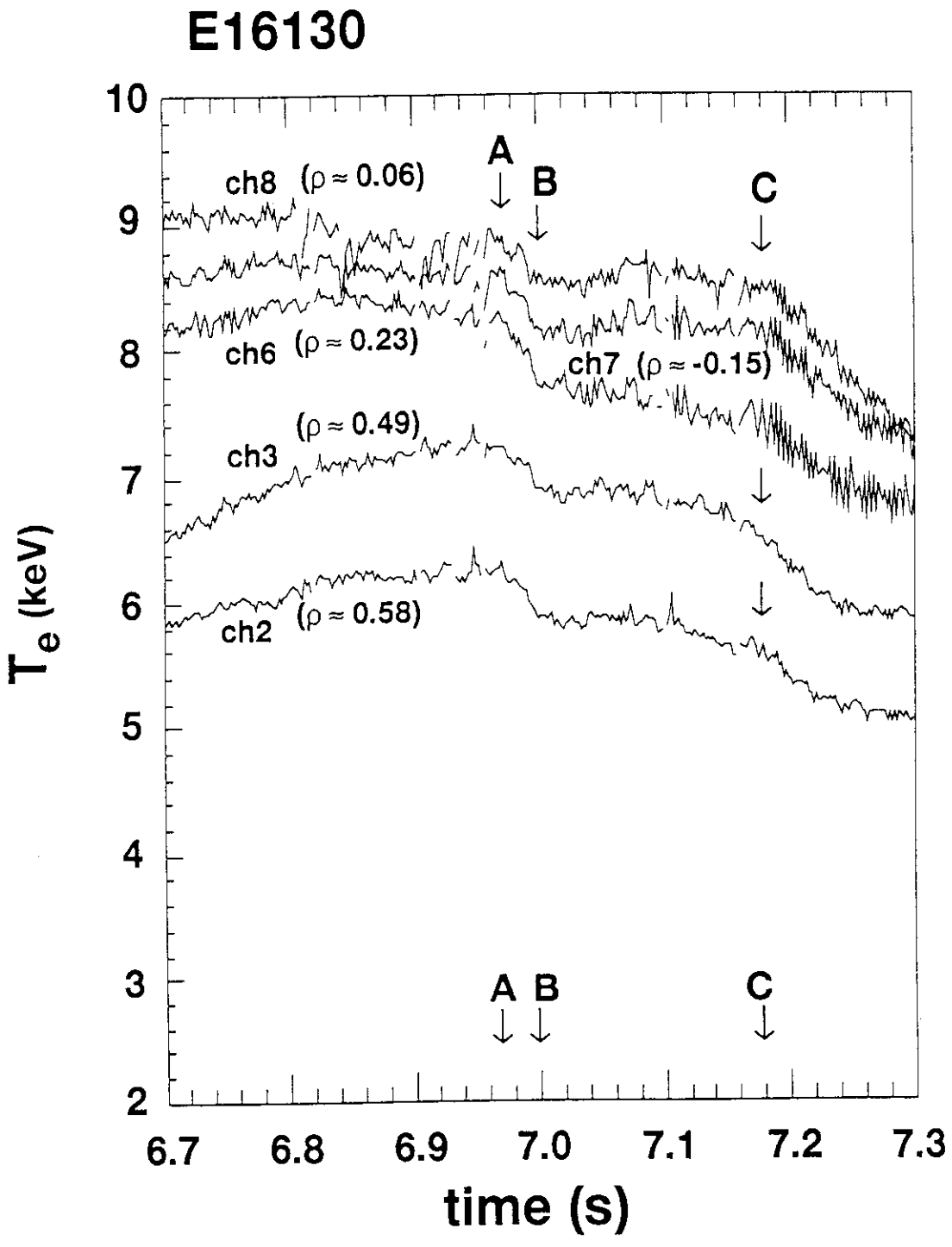


Fig. 3 Time evolution of $T_e(\rho, t)$ in the high field side for 16130 pulse. Evolutions of $T_e$ in both sides are basically the same with each other.

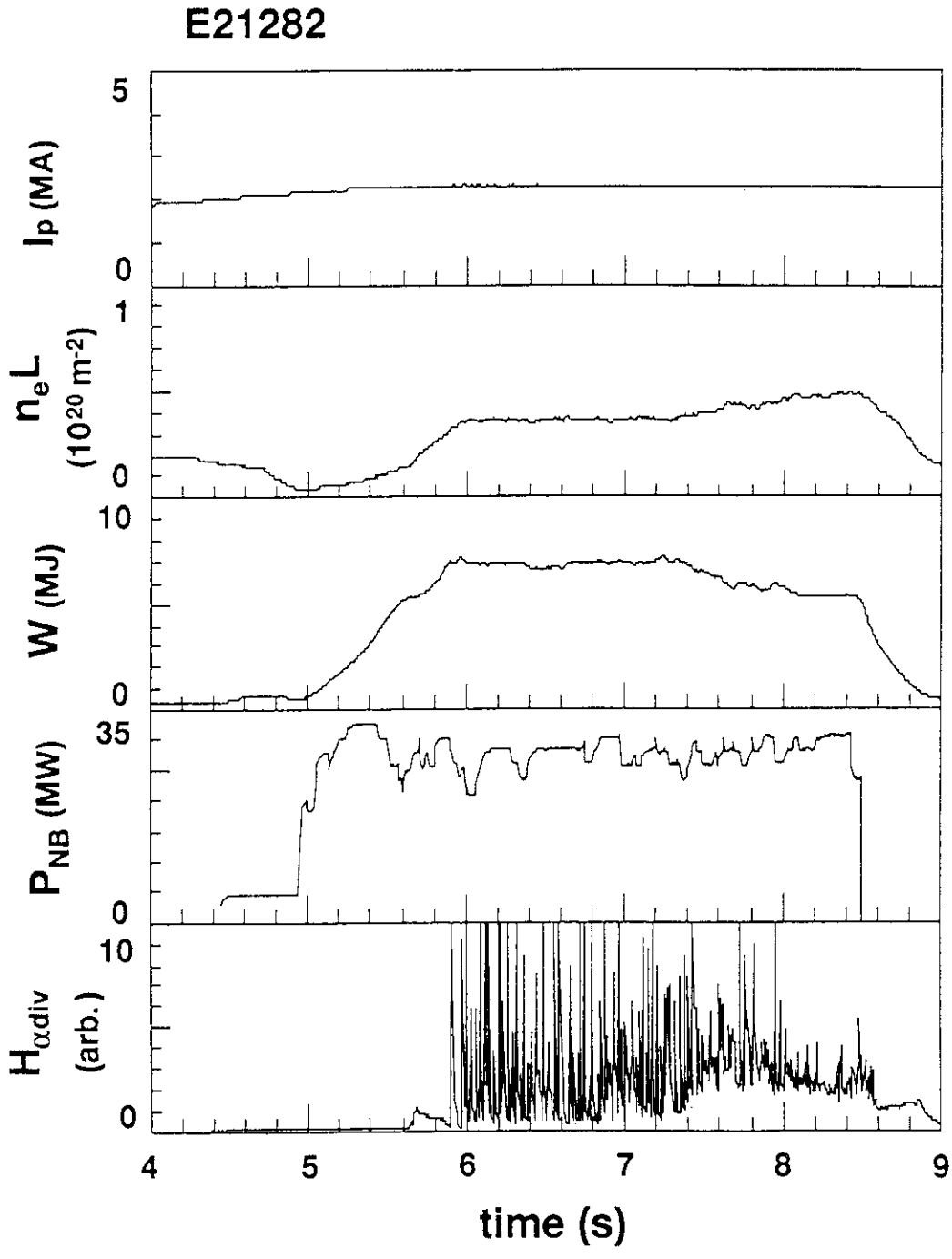


Fig. 4 Waveforms of a "steady-state high $\beta_p$ ELMy H mode" pulse 21282 (2.3 MA / 4.2 T and V ≈ 50 $m^3$). End of the "steady-state phase" is around 7.5 s.

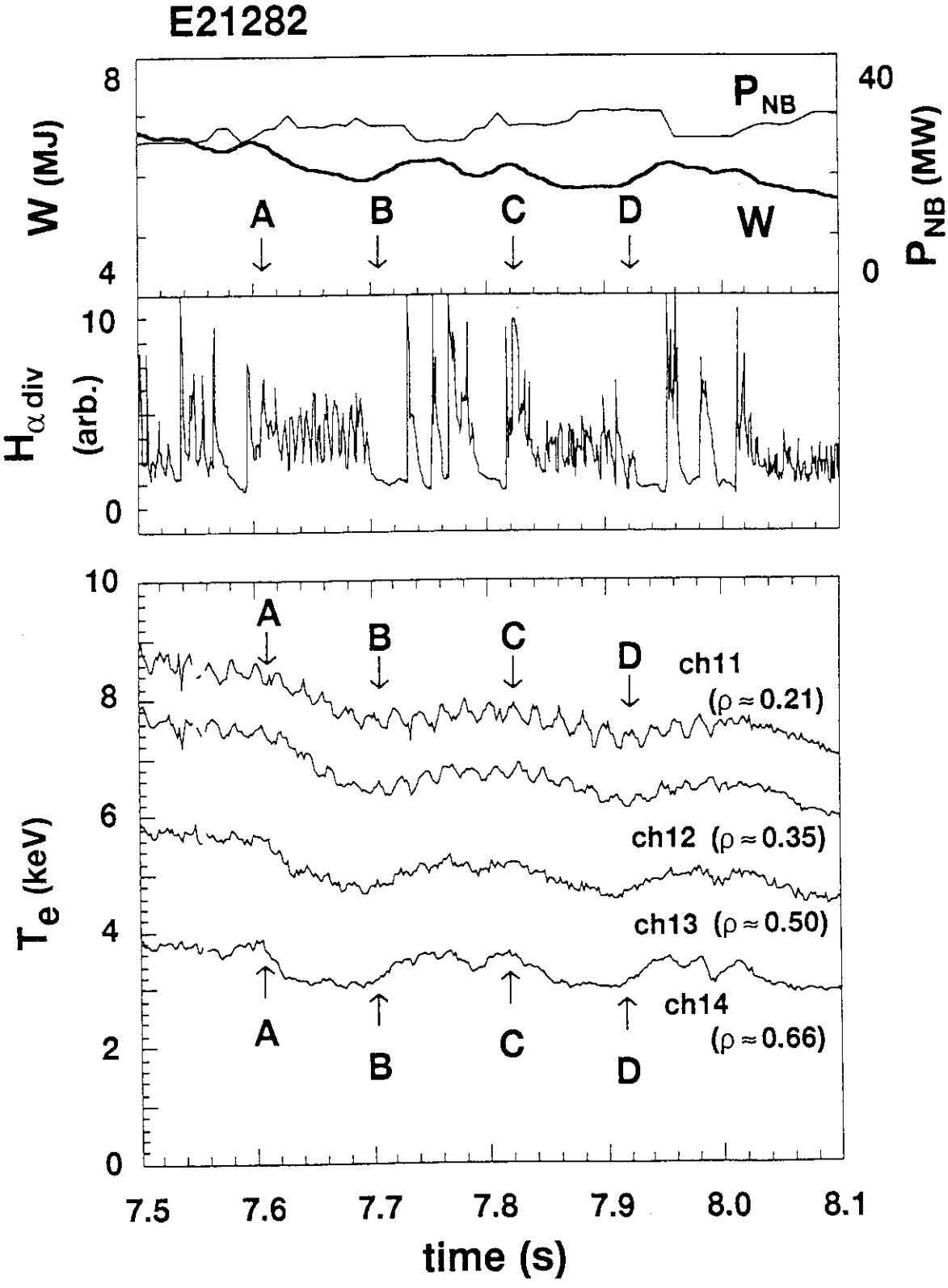


Fig. 5 Evolutions of W, $P_{NB}$, $H\alpha_{div}$, and $T_e(\rho, t)$, for 21282 pulse. Two L modes (A-B and C-D) with transitions back to H-mode are clearly observed on $H_\alpha$ and W signals. Time behaviours of $T_e(\rho=0.66)$ and $T_e(\rho=0.5)$ are similar to that of W. For the central region, $\rho$ = 0.35 and 0.21, however, the time delay of $T_e$ response is clearly seen.

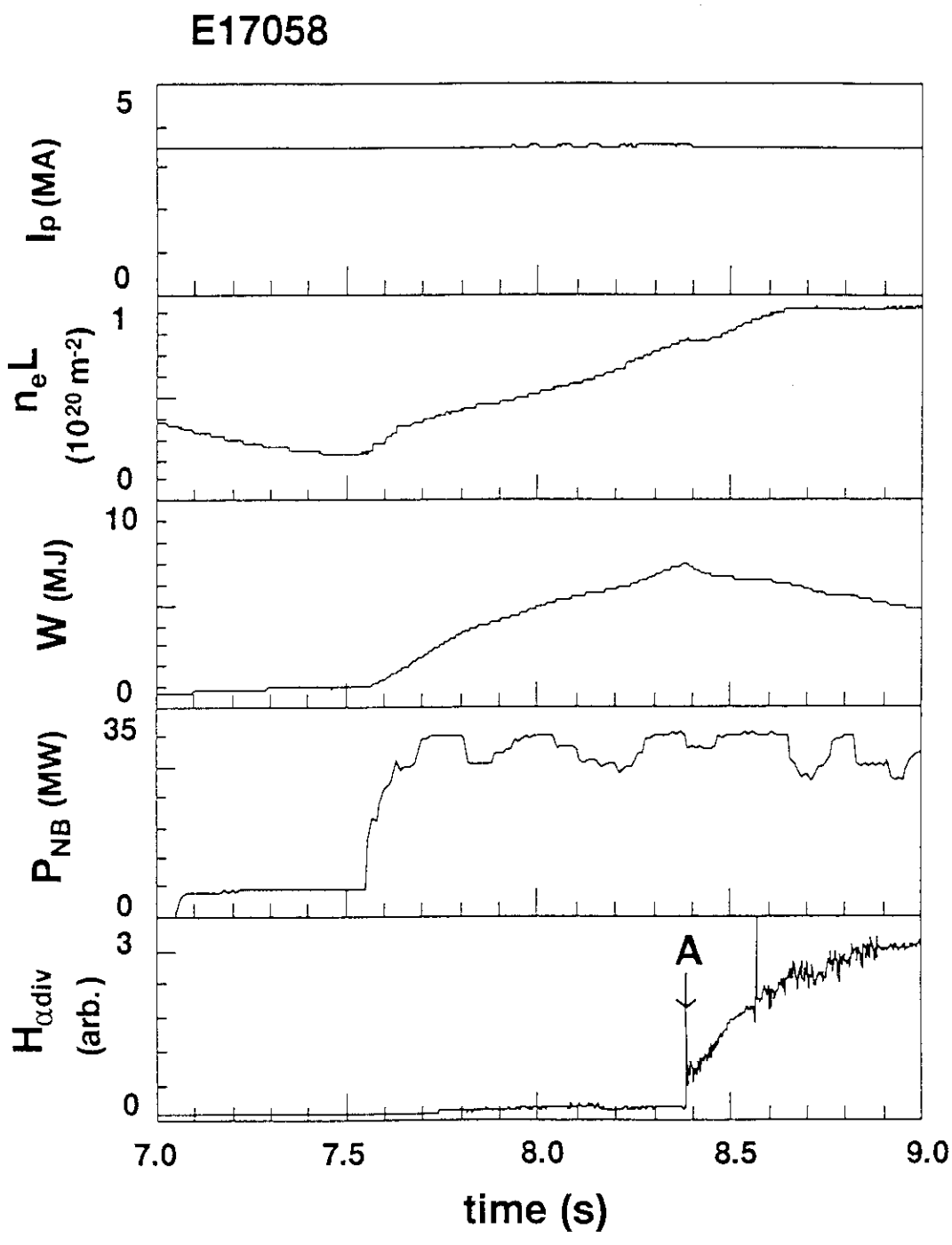


Fig. 6 Waveforms of a hot ion H mode pulse 17058 (3.5 MA/4.2 T). The growth of W is interrupted by a clear H-L transition at the time A and the improved confinement does not recover later.

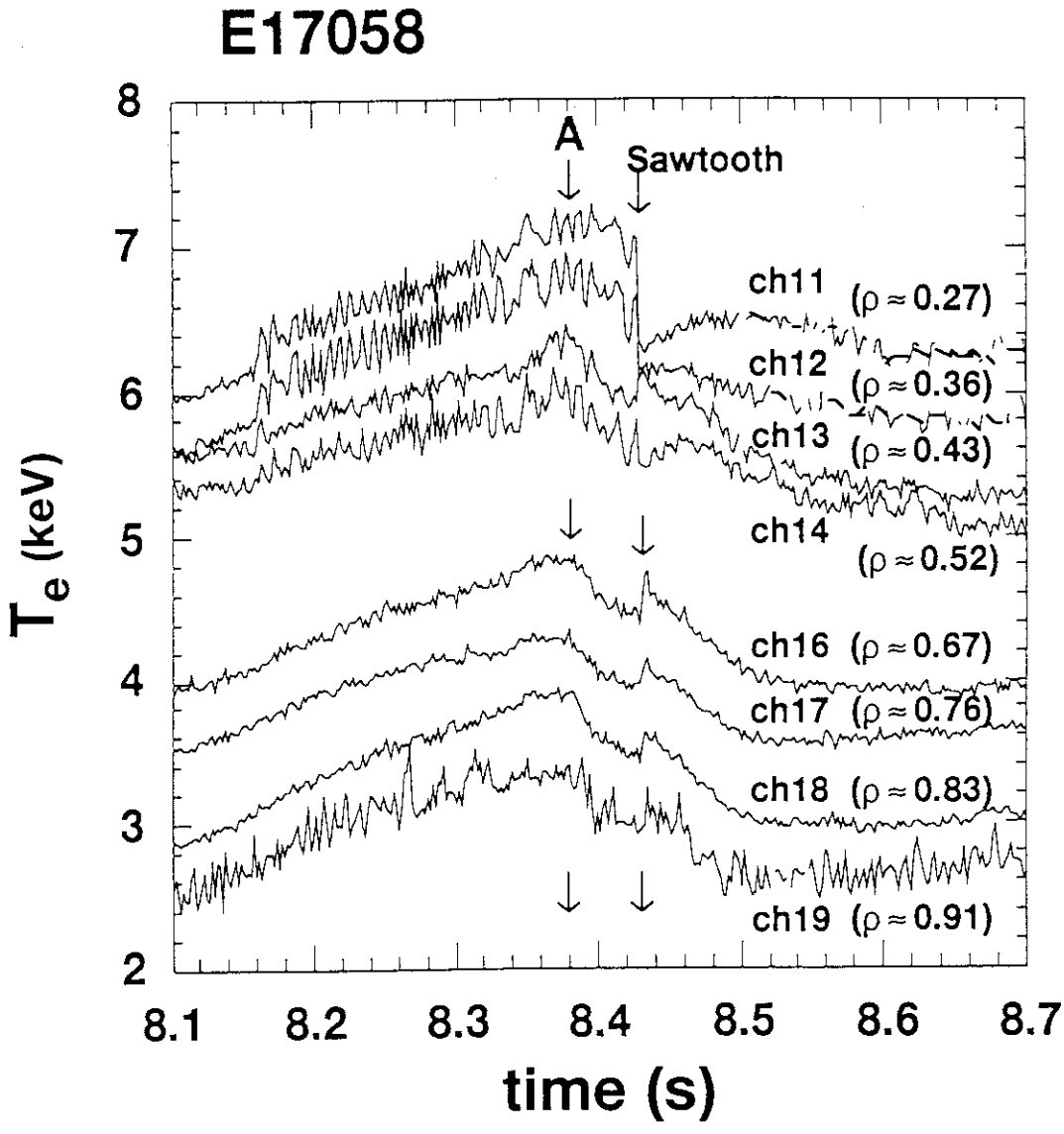


Fig. 7 Time evolution of $T_e(\rho, t)$ for 17058 pulse. Sawtooth crash occurs about 50 ms after the transition A. In the region, $0.43 < \rho < 0.83$, $T_e$ varies simultaneously after the transition, while in the central region, $\rho < 0.36$, $T_e$ is changed slowly.

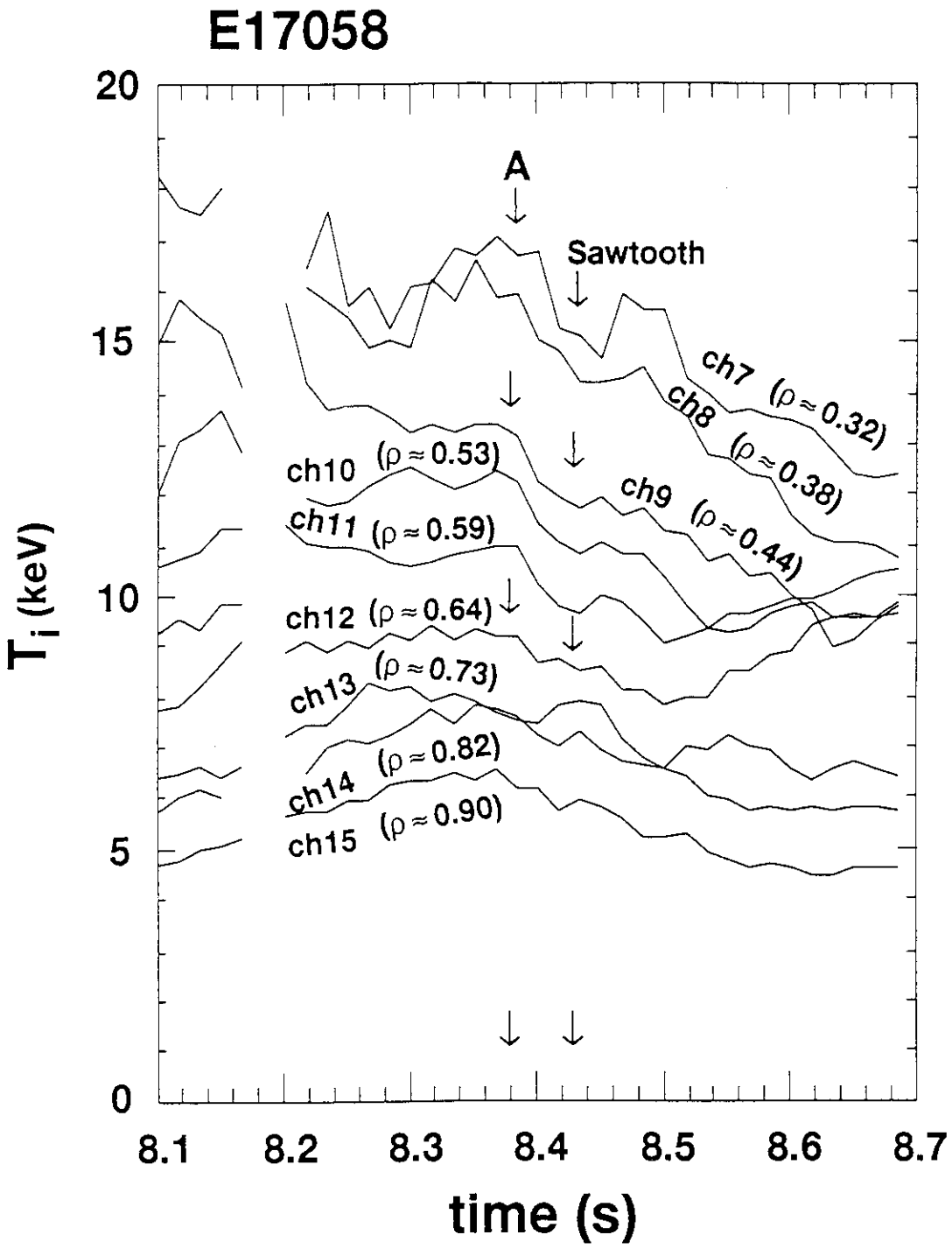


Fig. 8 Time evolution of ion temperature profile, $T_i(\rho, t)$, for 17058 pulse. $T_i(\rho, t)$ behaves similarly to $T_e(\rho, t)$.

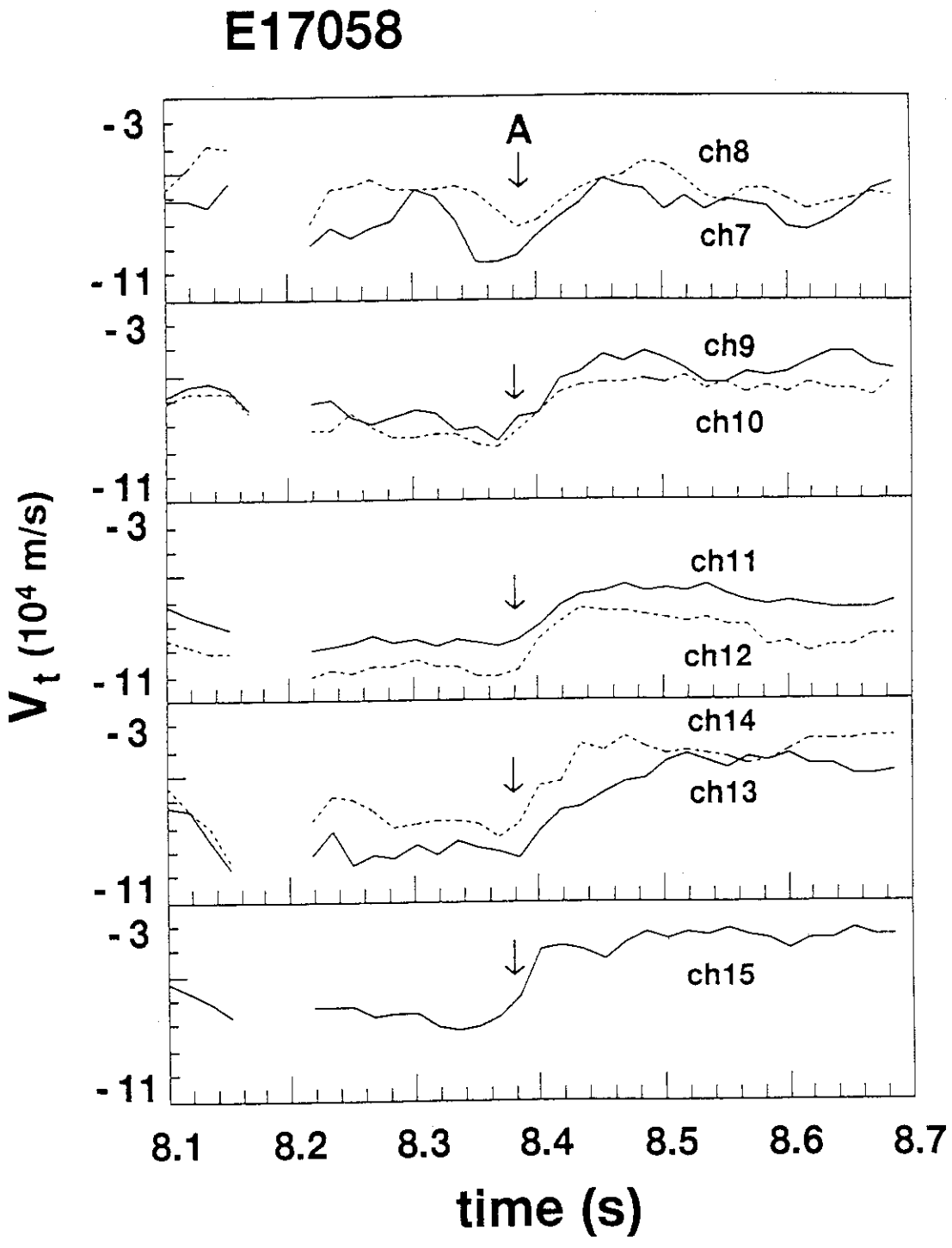


Fig. 9 Time evolution of toroidal rotation velocity, $V_t(\rho, t)$, for 17058 pulse. Clear correlation between $V_t(\rho, t)$ and $T_e(\rho, t)$ is seen.

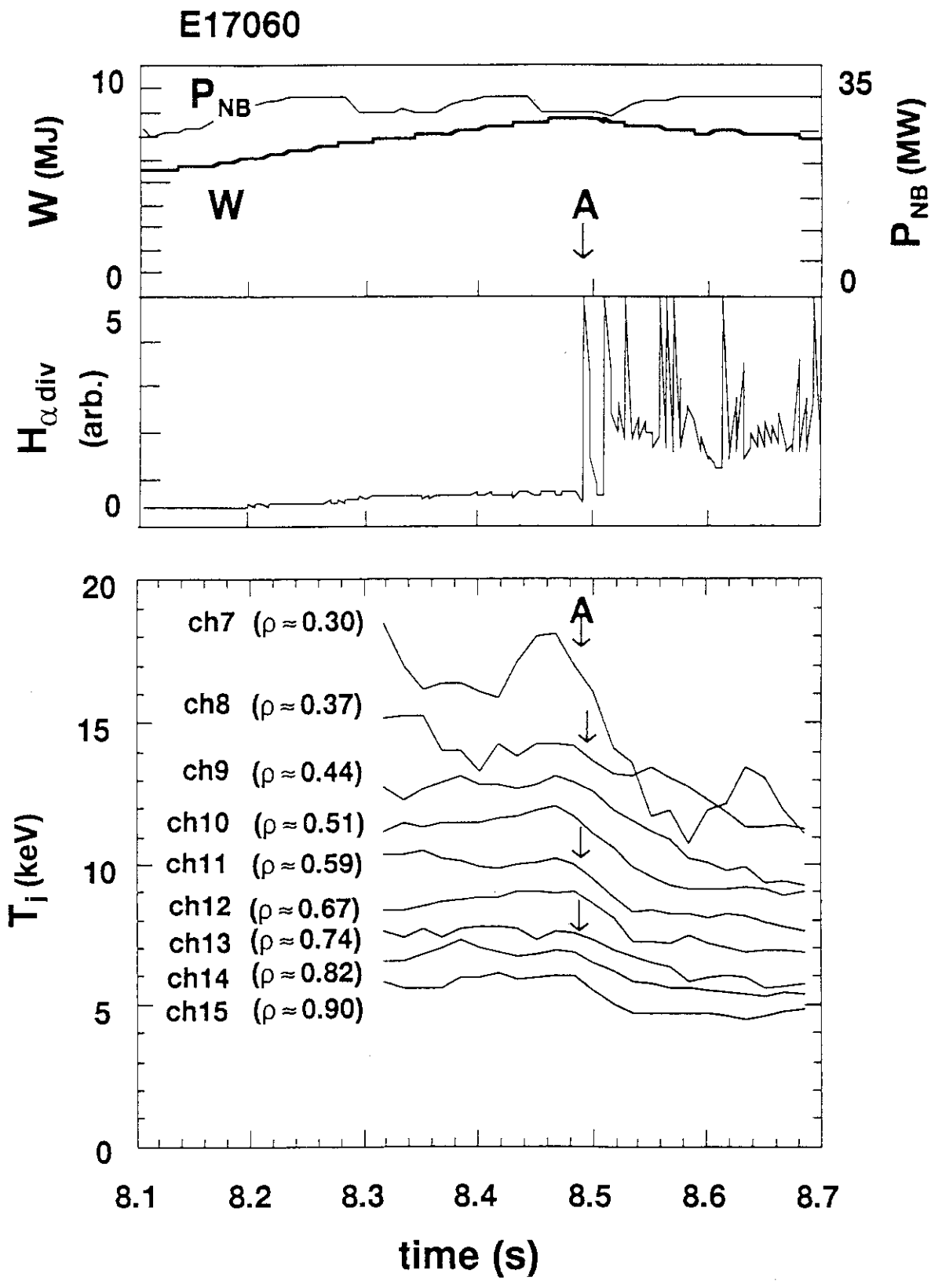


Fig. 10 Evolutions of W, $P_{NB}$, $H\alpha_{div}$, and $T_i(\rho, t)$, for a hot ion H-mode pulse 17060 (3.5 MA/4.2 T). Clear H-L transition is seen at the time A.

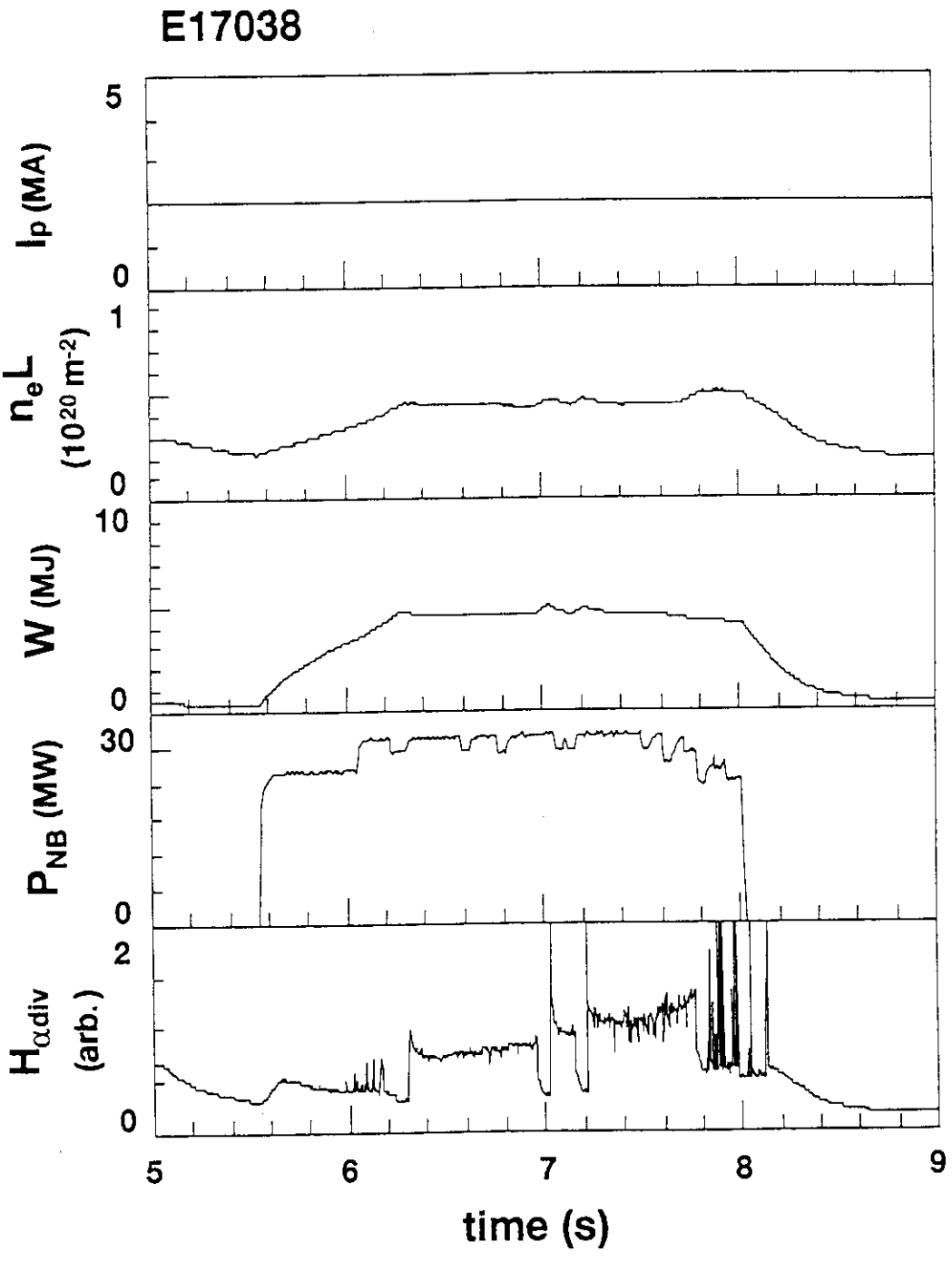


Fig. 11 Waveforms of a hot ion H mode pulse 17038 with low $I_p$ (2 MA/4.2 T). Two short H-mode phases are seen around 7 s.

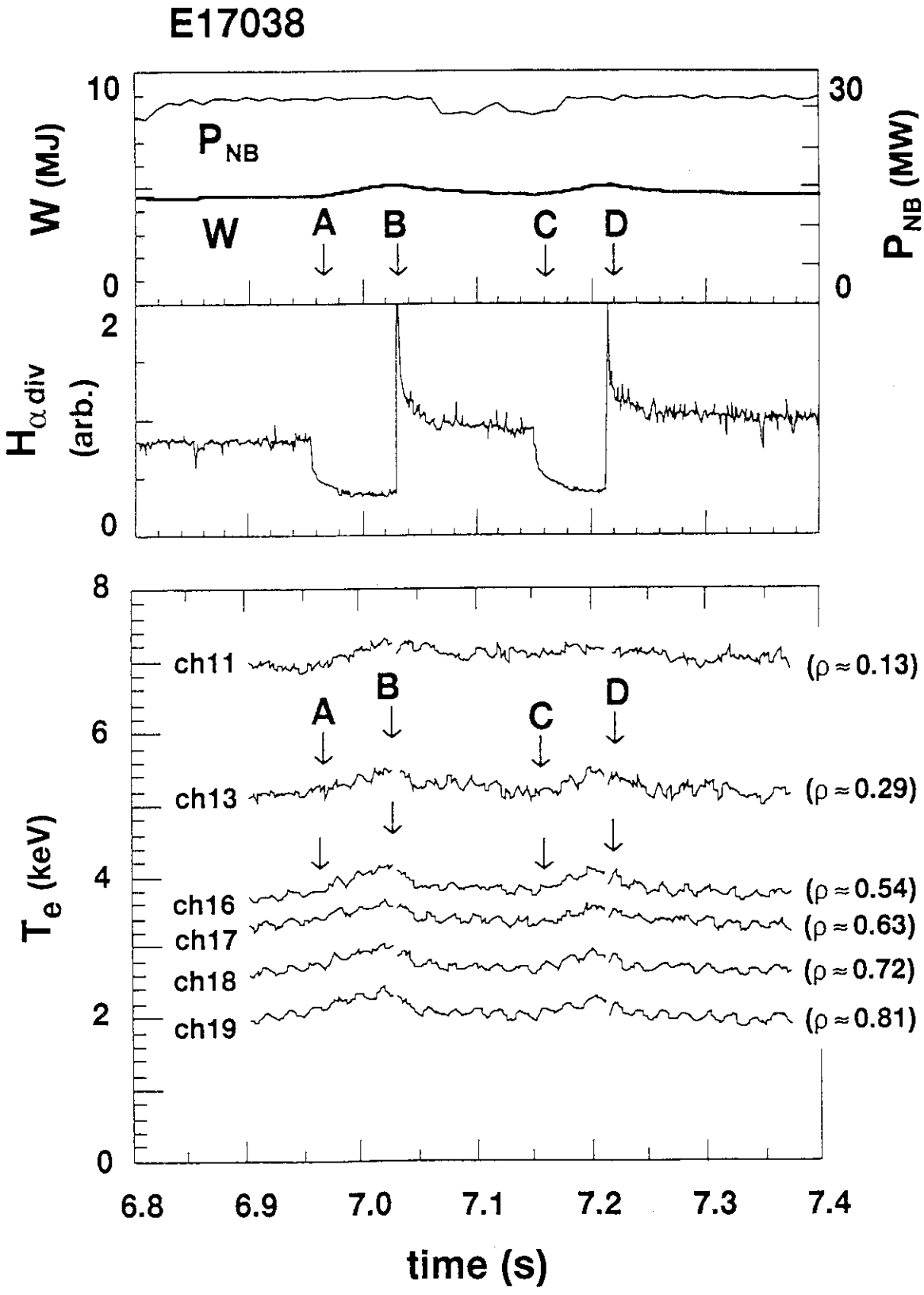


Fig. 12 Evolutions of W, $P_{NB}$, $H\alpha_{div}$, and $T_e(\rho, t)$, for 17038 pulse. Simultaneous response of $T_e$ over the wide region, $0.3 < \rho < 0.8$, with W and $H\alpha_{div}$ is clearly seen

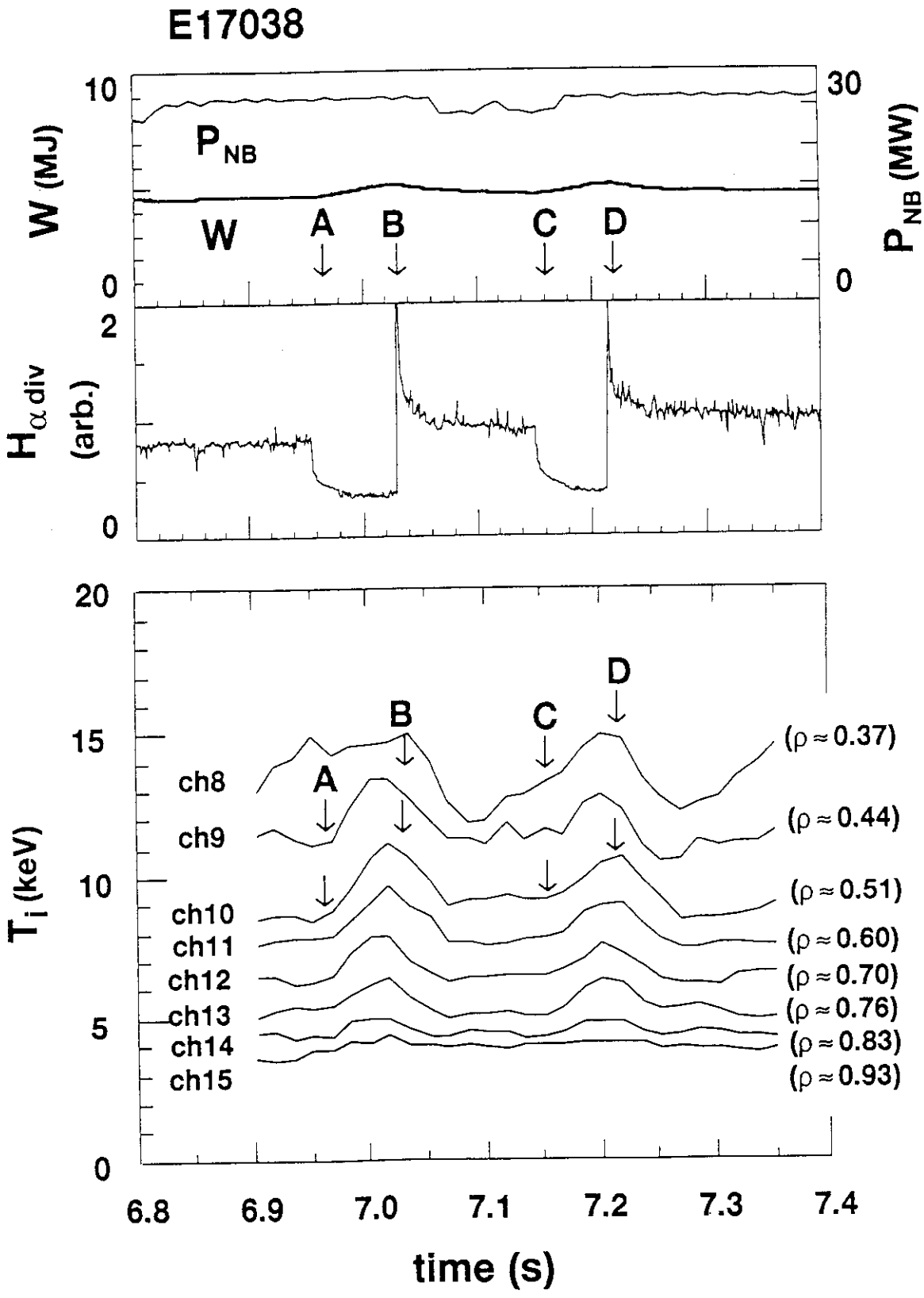


Fig. 13 Evolutions of W, $P_{NB}$, $H\alpha_{div}$, and $T_i(\rho, t)$, for 17038 pulse. Simultaneous response of $T_i$ over the wide region, $0.3 < \rho < 0.8$, is clearly seen as the same as $T_e(\rho, t)$.

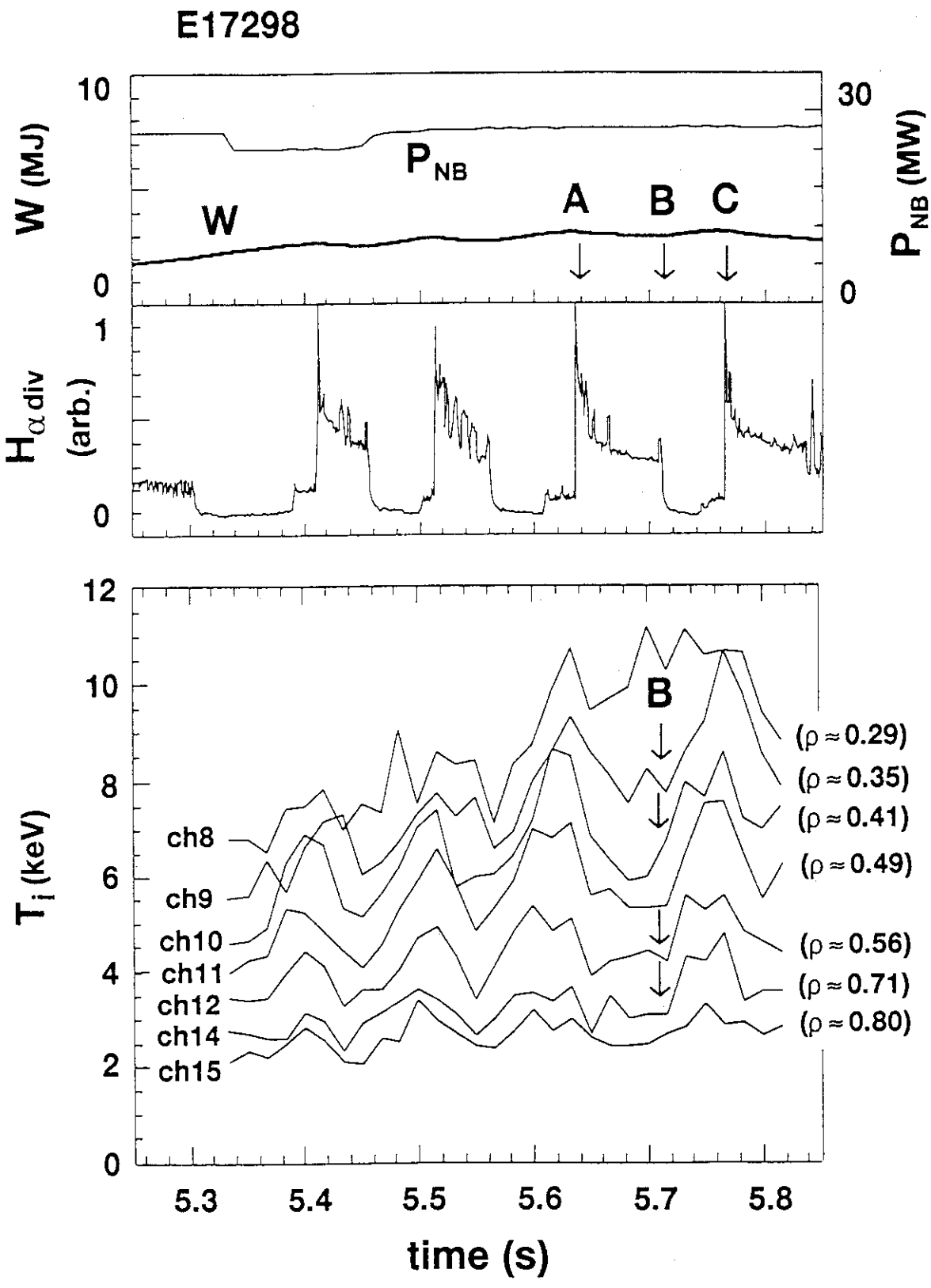


Fig. 14 Evolutions of W, $P_{NB}$, $H\alpha_{div}$, and $T_i(\rho, t)$, for a low field H-mode pulse 17298 (1.5 MA/2.5 T). Clear H-L-H-L transitions (A, B and C) are observed. Simultaneous response of $T_i$ over the wide region, $0.3 < \rho < 0.8$, is seen.

# Appendix Plasma configurations and parameters

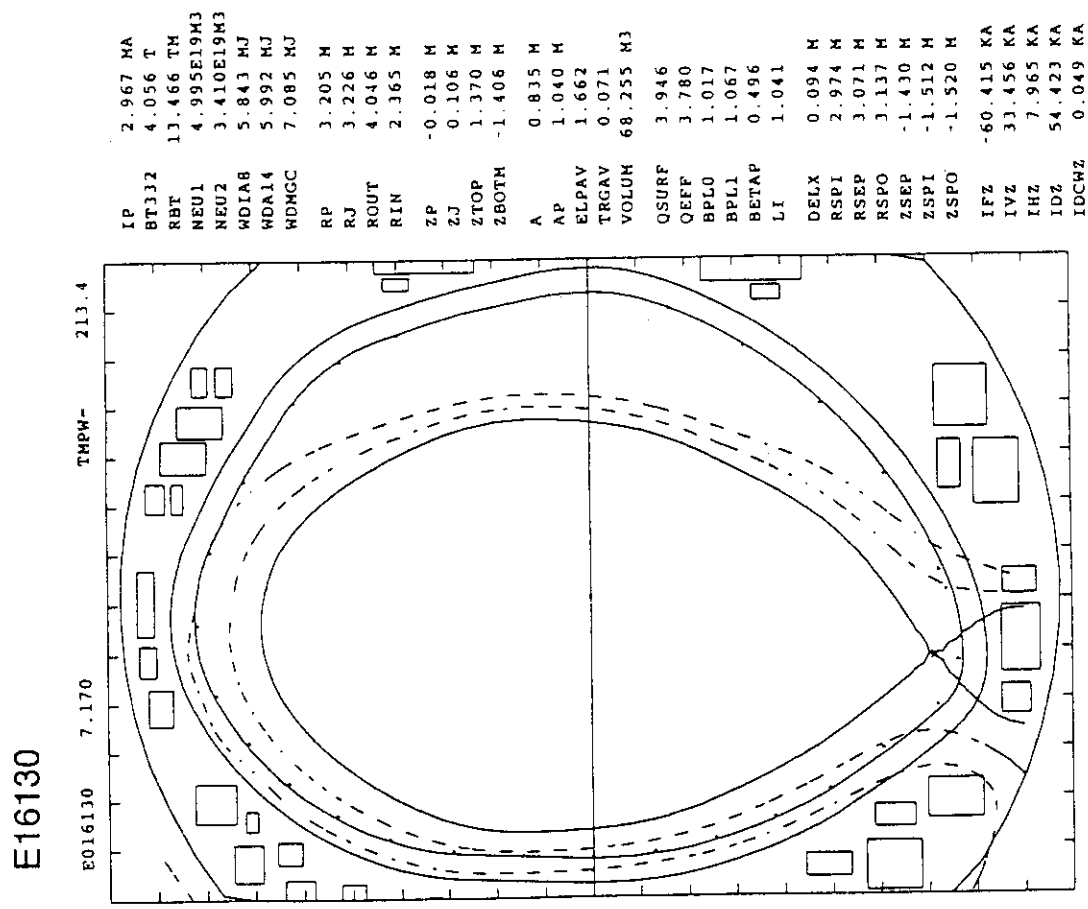


| | | | | | |
|---|---|---|---|---|---|
| IP | 2.967 MA | VLSM | -1.098 V | CRCM | 6.933 |
| BT332 | 4.056 T | PSURF | 0.434 V/S | | |
| RBT | 13.466 TM | | | CRCM1 | 7.033 |
| NEU1 | 4.995E19M3 | PBTOT | 19.993 MW | CNCL1 | 67.399 |
| NEU2 | 3.410E19M3 | PBCO | 15.722 MW | CNX11 | 1.595 |
| WDIA8 | 5.843 MJ | EBAVE | 88.026 KEV | CNX10 | 2.250 |
| WDA14 | 5.992 MJ | PBTCR | 0.000 MW | SLP11 | 0.037 |
| WDMGC | 7.085 MJ | PBTCO | 3.408 MW | SLP10 | 0.041 |
| | | PLHT | 0.000 MW | CRCM2 | 7.005 |
| RP | 3.205 M | PLHC | 0.000 MW | CNCL2 | 64.444 |
| RJ | 3.226 M | PIC | 0.000 MW | CNX21 | 0.489 |
| ROUT | 4.046 M | PIC1 | 0.000 MW | CNX20 | 1.522 |
| RIN | 2.365 M | | | SLP21 | 0.045 |
| | | Q1 | 0.000PM3/S | SLP20 | 0.053 |
| ZP | -0.018 M | Q2 | 0.000PM3/S | | |
| ZJ | 0.106 M | Q3 | 0.000PM3/S | CRCM3 | 6.984 |
| ZTOP | 1.370 M | Q4 | 0.000PM3/S | CNCL3 | 63.265 |
| ZBOTM | -1.406 M | | | CNX31 | 0.000 |
| | | DL 0 | 52.943 CM | CNX30 | 1.145 |
| A | 0.835 M | DL 7 | 50.783 CM | SLP31 | 0.052 |
| AP | 1.040 M | DL 16 | 47.631 CM | SLP30 | 0.061 |
| ELPAV | 1.662 | DL 37 | 44.918 CM | | |
| TRGAV | 0.071 | DL 47 | 44.827 CM | RSP11 | 2.920 |
| VOLUM | 68.255 M3 | DL 57 | 39.693 CM | RSP21 | 2.879 |
| | | DL 71 | 28.254 CM | RSP31 | 2.839 |
| QSURF | 3.946 | DL 93 | 26.157 CM | | |
| QEFF | 3.780 | DL112 | 21.497 CM | RSP10 | 3.195 |
| BPL0 | 1.017 | DL150 | 11.381 CM | RSP20 | 3.238 |
| BPL1 | 1.067 | DL180 | 11.103 CM | RSP30 | 3.275 |
| BETAP | 0.496 | DL207 | 14.915 CM | | |
| LI | 1.041 | DL292 | 30.597 CM | BZSP1 | -0.103 |
| | | DL309 | 39.544 CM | BTSP1 | 4.528 |
| DELX | 0.094 M | DL328 | 46.843 CM | BZ/T1 | -0.023 |
| RSPI | 2.974 M | DL344 | 51.341 CM | BZSP2 | 0.115 |
| RSEP | 3.071 M | | | BTSP2 | 4.293 |
| RSPO | 3.137 M | LU1 | 1.963 M | BZ/T2 | 0.027 |
| ZSEP | -1.430 M | LU2 | 2.319 M | | |
| ZSPI | -1.512 M | | | ALNE | -0.859 |
| ZSPO | -1.520 M | SL1 | 1.026 | DEN0 | 0.710 |
| | | SL2 | 0.503 | DENAV | 2.982 |
| IFZ | -60.415 KA | | | IP | 2.967 |
| IVZ | 33.456 KA | DRZ | -0.113 M | RKC03 | 0.000 |
| IHZ | 7.965 KA | D2Z | 0.067 M | RKC11 | 2.989 |
| IDZ | 54.423 KA | DELXZ | 0.088 M | IPUNC | 2.967 |
| IDCWZ | 0.049 KA | TRIGZ | 0.000 | PRTOT | 0.000 |
| | | | | PRMAI | 0.000 |
| NINDX | -1.548 | | | PRDIV | 0.000 |
| NS | 0.000 | | | QSTAR | 2.920 |
| | | | | NEUT2 | 0.000E+00 |
| BPCHI | 1.439E-01 | | | | |
| BPCHO | 2.165E-01 | | | | |

# E21282

E021282 7.920 TMPW= 269.0

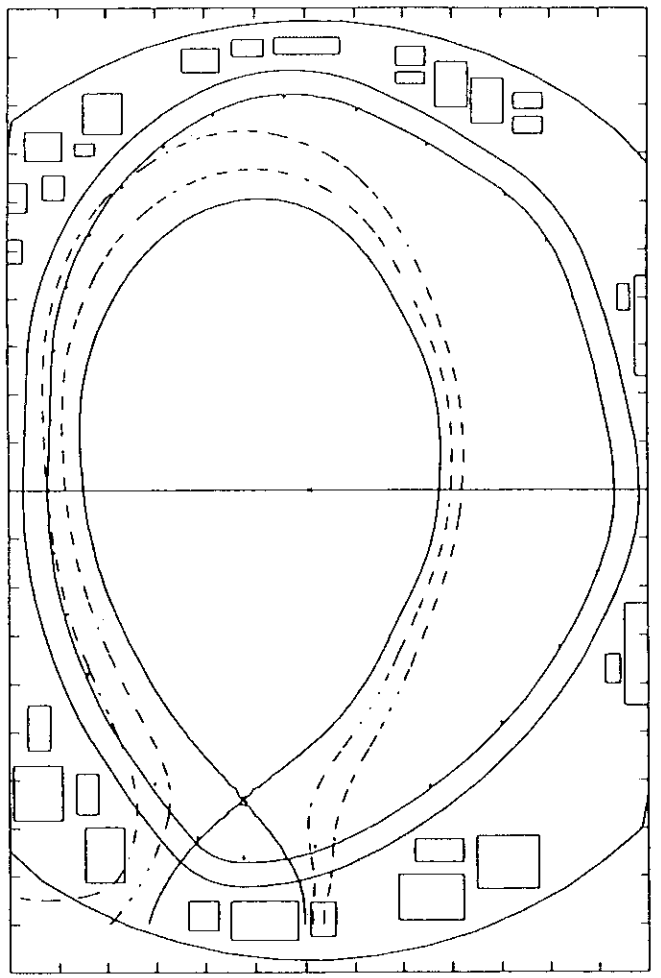

| | | |
|---|---|---|
| IP | 2.264 | MA |
| BT332 | 4.005 | T |
| RBT | 13.296 | TM |
| NEU1 | 2.547E19 | M3 |
| NEU2 | 2.494E19 | M3 |
| WDIA8 | 5.746 | MJ |
| WDA14 | 5.747 | MJ |
| WDMGC | 6.388 | MJ |
| RP | 3.125 | M |
| RJ | 3.162 | M |
| ROUT | 3.855 | M |
| RIN | 2.391 | M |
| ZP | -0.024 | M |
| ZJ | 0.089 | M |
| ZTOP | 1.212 | M |
| ZBOTM | -1.260 | M |
| A | 0.728 | M |
| AP | 0.915 | M |
| ELPAV | 1.697 | |
| TRGAV | 0.055 | |
| VOLUM | 51.459 | M3 |
| QSURF | 4.257 | |
| QEFF | 4.075 | |
| BPL0 | 1.313 | |
| BPL1 | 1.370 | |
| BETAP | 0.867 | |
| LI | 0.891 | |
| DELX | 0.241 | M |
| RSPI | 2.875 | M |
| RSEP | 3.049 | M |
| RSPO | 3.217 | M |
| ZSEP | -1.282 | M |
| ZSPI | -1.448 | M |
| ZSPO | -1.508 | M |
| IFZ | -41.006 | KA |
| IVZ | 31.474 | KA |
| IHZ | 15.847 | KA |
| IDZ | 84.497 | KA |
| IDCWZ | 0.039 | KA |
| NINDX | -1.802 | |
| NS | 0.000 | |
| BPCHI | 1.211E-01 | |
| BPCHO | 1.860E-01 | |

| | | |
|---|---|---|
| VLSM | 1.170 | V |
| PSURF | 0.162 | VS |
| PBTOT | 30.632 | MW |
| PBCO | 18.817 | MW |
| EBAVE | 87.934 | KEV |
| PBTCR | 4.722 | MW |
| PBTCO | 4.573 | MW |
| PLHT | 0.000 | MW |
| PLHC | 0.000 | MW |
| PIC | 0.000 | MW |
| PIC1 | 0.000 | MW |
| Q1 | 0.000 | PM3/S |
| Q2 | 0.000 | PM3/S |
| Q3 | 0.000 | PM3/S |
| Q4 | 0.000 | PM3/S |
| DL 0 | 71.484 | CM |
| DL 7 | 69.798 | CM |
| DL 16 | 67.114 | CM |
| DL 37 | 65.436 | CM |
| DL 47 | 65.610 | CM |
| DL 57 | 60.457 | CM |
| DL 71 | 48.779 | CM |
| DL 93 | 42.589 | CM |
| DL112 | 30.748 | CM |
| DL150 | 14.635 | CM |
| DL180 | 13.893 | CM |
| DL207 | 19.049 | CM |
| DL292 | 46.831 | CM |
| DL309 | 56.159 | CM |
| DL328 | 63.779 | CM |
| DL344 | 68.953 | CM |
| LU1 | 1.785 | M |
| LU2 | 1.767 | M |
| SL1 | 1.043 | |
| SL2 | 0.792 | |
| DRZ | -0.282 | M |
| DZZ | -0.060 | M |
| DELXZ | 0.419 | M |
| TRIGZ | 0.000 | |

| | |
|---|---|
| CRCM | 6.126 |
| CRCM1 | 6.477 |
| CNCL1 | 75.332 |
| CNX1I | 3.966 |
| CNX1O | 5.375 |
| SLP1I | 0.043 |
| SLP1O | 0.074 |
| CRCM2 | 6.445 |
| CNCL2 | 71.449 |
| CNX2I | 2.509 |
| CNX2O | 4.208 |
| SLP2I | 0.047 |
| SLP2O | 0.077 |
| CRCM3 | 6.439 |
| CNCL3 | 70.290 |
| CNX3I | 1.611 |
| CNX3O | 3.597 |
| SLP3I | 0.049 |
| SLP3O | 0.081 |
| RSP1I | 2.852 |
| RSP2I | 2.828 |
| RSP3I | 2.803 |
| RSP1O | 3.240 |
| RSP2O | 3.262 |
| RSP3O | 3.283 |
| BZSP1 | -0.191 |
| BTSP1 | 4.625 |
| BZ/T1 | -0.041 |
| BZSP2 | 0.286 |
| BTSP2 | 4.133 |
| BZ/T2 | 0.069 |
| ALNE | -0.055 |
| DEN0 | 2.369 |
| DENAV | 2.453 |
| IP | 2.264 |
| RKC03 | 0.000 |
| RKC11 | 2.264 |
| IPUNC | 2.246 |
| PRTOT | 16.747 |
| PRMAI | 6.064 |
| PRDIV | 10.683 |
| QSTAR | 3.109 |

NEUT2 0.000E+00

95-07-17 16:01:17
VER.9.0IP-RKC3,11

| | |
|---|---|
| T-PROB FITTING - | 1 |
| N-PROB FITTING - | 0 |
| FLUX FITTING - | 1 |
| NO. OF FILAMENT - | 6 |

NORM-SIGM
T- 5.084E-03
P- 2.677E-04
N- 6.769E-03
HIGH ELONG.

# E17058

E017058 8.380 TMPW= 148.1

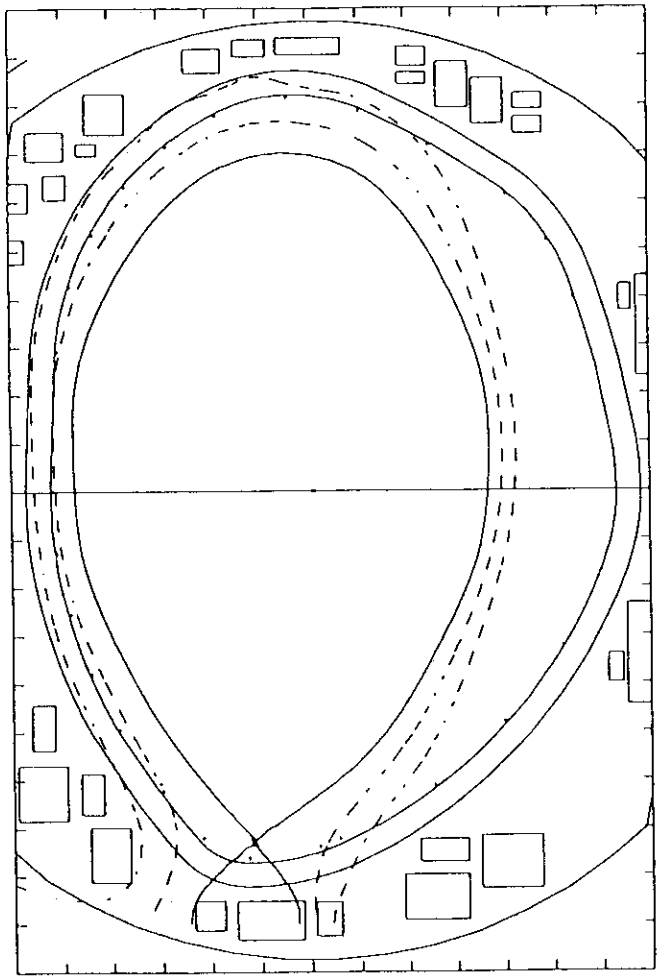

| | | |
|---|---|---|
| IP | 3.496 | MA |
| BT332 | 4.088 | T |
| RBT | 13.573 | TM |
| NEU1 | 2.929E19 | M3 |
| NEU2 | 3.270E19 | M3 |
| WDIA8 | 6.815 | MJ |
| WDA14 | 6.965 | MJ |
| WDMGC | 8.677 | MJ |
| RP | 3.196 | M |
| RJ | 3.206 | M |
| ROUT | 4.044 | M |
| RIN | 2.350 | M |
| ZP | -0.017 | M |
| ZJ | 0.100 | M |
| ZTOP | 1.400 | M |
| ZBOTM | -1.434 | M |
| A | 0.845 | M |
| AP | 1.056 | M |
| ELPAV | 1.676 | |
| TRGAV | 0.059 | |
| VOLUM | 70.194 | M3 |
| QSURF | 3.481 | |
| QEFF | 3.371 | |
| BPL0 | 0.900 | |
| BPL1 | 0.956 | |
| BETAP | 0.419 | |
| LI | 0.962 | |
| DELX | 0.066 | M |
| RSPI | 3.000 | M |
| RSEP | 3.070 | M |
| RSPO | 3.117 | M |
| ZSEP | -1.457 | M |
| ZSPI | -1.519 | M |
| ZSPO | -1.522 | M |
| IFZ | -62.878 | KA |
| IVZ | 38.590 | KA |
| IHZ | 7.647 | KA |
| IDZ | 59.776 | KA |
| IDCWZ | 0.013 | KA |
| NINDX | -1.545 | |
| NS | 0.000 | |
| BPCHI | 1.650E-01 | |
| BPCHO | 2.395E-01 | |

| | | |
|---|---|---|
| VLSM | -0.478 | V |
| PSURF | 0.285 | VS |
| PBTOT | 30.356 | MW |
| PBCO | 18.652 | MW |
| EBAVE | 88.093 | KEV |
| PBTCR | 4.649 | MW |
| PBTCO | 4.362 | MW |
| PLHT | 0.000 | MW |
| PLHC | 0.000 | MW |
| PIC | 0.000 | MW |
| PIC1 | 0.000 | MW |
| Q1 | 0.000 | PM3/S |
| Q2 | 0.000 | PM3/S |
| Q3 | 0.000 | PM3/S |
| Q4 | 0.000 | PM3/S |
| DL 0 | 52.709 | CM |
| DL 7 | 50.923 | CM |
| DL 16 | 48.050 | CM |
| DL 37 | 45.400 | CM |
| DL 47 | 45.039 | CM |
| DL 57 | 39.377 | CM |
| DL 71 | 26.858 | CM |
| DL 93 | 23.184 | CM |
| DL112 | 18.735 | CM |
| DL150 | 10.200 | CM |
| DL180 | 8.969 | CM |
| DL207 | 12.047 | CM |
| DL292 | 29.421 | CM |
| DL309 | 38.663 | CM |
| DL328 | 45.606 | CM |
| DL344 | 50.432 | CM |
| LU1 | 2.039 | M |
| LU2 | 2.359 | M |
| SL1 | 1.019 | |
| SL2 | 0.390 | |
| DRZ | -0.114 | M |
| DZZ | 0.068 | M |
| DELXZ | 0.078 | M |
| TRIGZ | 0.000 | |

| | |
|---|---|
| CRCM | 7.049 |
| CRCM1 | 7.100 |
| CNCL1 | 58.606 |
| CNX1I | 0.917 |
| CNX1O | 1.402 |
| SLP1I | 0.039 |
| SLP1O | 0.042 |
| CRCM2 | 7.073 |
| CNCL2 | 56.353 |
| CNX2I | 0.033 |
| CNX2O | 0.879 |
| SLP2I | 0.050 |
| SLP2O | 0.056 |
| CRCM3 | 7.044 |
| CNCL3 | 55.195 |
| CNX3I | 0.000 |
| CNX3O | 0.602 |
| SLP3I | 0.057 |
| SLP3O | 0.066 |
| RSP1I | 2.933 |
| RSP2I | 2.886 |
| RSP3I | 2.841 |
| RSP1O | 3.186 |
| RSP2O | 3.233 |
| RSP3O | 3.273 |
| BZSP1 | -0.085 |
| BTSP1 | 4.524 |
| BZ/T1 | -0.019 |
| BZSP2 | 0.093 |
| BTSP2 | 4.355 |
| BZ/T2 | 0.021 |
| ALNE | 0.333 |
| DEN0 | 4.124 |
| DENAV | 3.470 |
| IP | 3.496 |
| RKC03 | 0.000 |
| RKC11 | 3.496 |
| IPUNC | 3.525 |
| PRTOT | 9.897 |
| PRMAI | 7.366 |
| PRDIV | 2.531 |
| QSTAR | 2.600 |

NEUT2 1.555E+16

95-07-17 16:04:53
VER.9.0IP-RKC3,11

| | |
|---|---|
| T-PROB FITTING - | 1 |
| N-PROB FITTING - | 0 |
| FLUX FITTING - | 1 |
| NO. OF FILAMENT - | 6 |

NORM-SIGM
T= 6.046E-03
P= 5.295E-04
N= 8.846E-02
HIGH ELONG.

# E17060

E017060 8.480 TMPW= 143.1

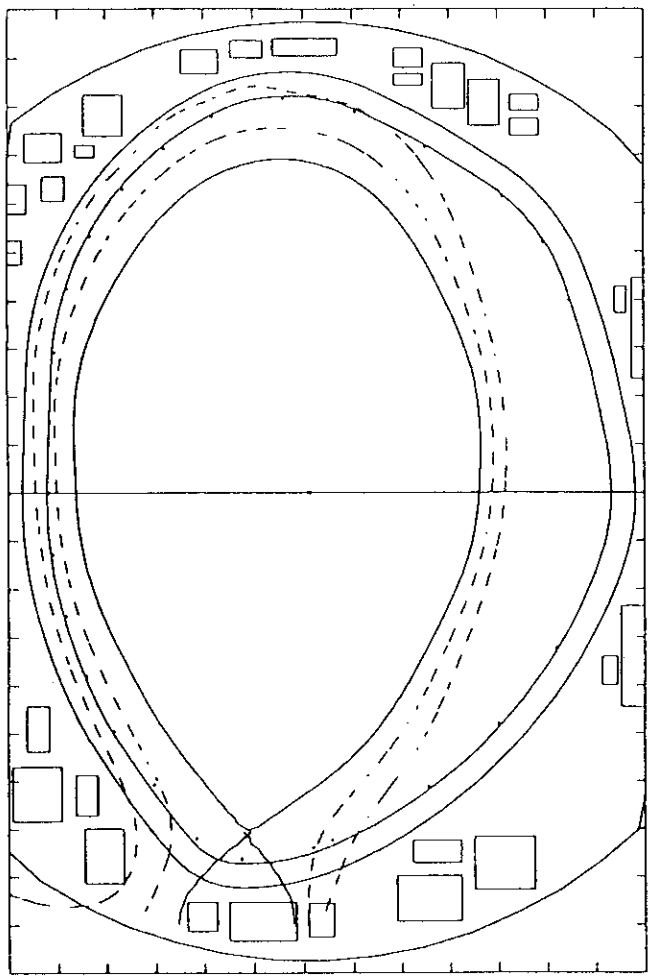

95-07-17 16:07:57
VER.9.0IP-RKC3,11

| | |
|---|---|
| T-PROB FITTING - | 1 |
| N-PROB FITTING - | 0 |
| FLUX FITTING - | 1 |
| NO. OF FILAMENT - | 6 |

NORM-SIGM
T= 4.419E-03
P= 3.971E-04
N= 8.675E-02
HIGH ELONG.

| | | |
|---|---|---|
| IP | 3.495 | MA |
| BT332 | 4.087 | T |
| RBT | 13.570 | TM |
| NEU1 | 2.957E19 | M3 |
| NEU2 | 3.302E19 | M3 |
| WDIA8 | 7.638 | MJ |
| WDA14 | 7.793 | MJ |
| WDMGC | 9.480 | MJ |
| RP | 3.198 | M |
| RJ | 3.212 | M |
| ROUT | 4.028 | M |
| RIN | 2.368 | M |
| ZP | -0.010 | M |
| ZJ | 0.106 | M |
| ZTOP | 1.381 | M |
| ZBOTM | -1.402 | M |
| A | 0.828 | M |
| AP | 1.036 | M |
| ELPAV | 1.681 | |
| TRGAV | 0.062 | |
| VOLUM | 67.516 | M3 |
| QSURF | 3.345 | |
| QEFF | 3.247 | |
| BPL0 | 0.947 | |
| BPL1 | 1.005 | |
| BETAP | 0.470 | |
| LI | 0.954 | |
| DELX | 0.098 | M |
| RSPI | 2.973 | M |
| RSEP | 3.072 | M |
| RSPO | 3.141 | M |
| ZSEP | -1.426 | M |
| ZSPI | -1.511 | M |
| ZSPO | -1.520 | M |
| IFZ | -62.917 | KA |
| IVZ | 39.322 | KA |
| IHZ | 9.964 | KA |
| IDZ | 70.250 | KA |
| IDCWZ | 0.013 | KA |
| NINDX | -1.583 | |
| NS | 0.000 | |
| BPCHI | 1.676E-01 | |
| BPCHO | 2.448E-01 | |

| | | |
|---|---|---|
| VLSM | 0.359 | V |
| PSURF | 0.254 | VS |
| PBTOT | 27.821 | MW |
| PBCO | 16.252 | MW |
| EBAVE | 89.462 | KEV |
| PBTCR | 4.655 | MW |
| PBTCO | 4.385 | MW |
| PLHT | 0.000 | MW |
| PLHC | 0.000 | MW |
| PIC | 0.000 | MW |
| PIC1 | 0.000 | MW |
| Q1 | 0.000 | PM3/S |
| Q2 | 0.000 | PM3/S |
| Q3 | 0.000 | PM3/S |
| Q4 | 0.000 | PM3/S |
| DL 0 | 54.327 | CM |
| DL 7 | 52.524 | CM |
| DL 16 | 49.622 | CM |
| DL 37 | 46.961 | CM |
| DL 47 | 46.594 | CM |
| DL 57 | 40.939 | CM |
| DL 71 | 28.532 | CM |
| DL 93 | 25.099 | CM |
| DL112 | 20.507 | CM |
| DL150 | 11.936 | CM |
| DL180 | 10.940 | CM |
| DL207 | 14.504 | CM |
| DL292 | 31.557 | CM |
| DL309 | 40.606 | CM |
| DL328 | 47.521 | CM |
| DL344 | 52.165 | CM |
| LU1 | 1.968 | M |
| LU2 | 2.306 | M |
| SL1 | 1.021 | |
| SL2 | 0.436 | |
| DRZ | -0.115 | M |
| DZZ | 0.068 | M |
| DELXZ | 0.098 | M |
| TRIGZ | 0.000 | |

| | | |
|---|---|---|
| CRCM | 6.917 | |
| CRCM1 | 7.029 | |
| CNCL1 | 57.595 | |
| CNX1I | 1.498 | |
| CNX1O | 2.022 | |
| SLP1I | 0.042 | |
| SLP1O | 0.049 | |
| CRCM2 | 7.003 | |
| CNCL2 | 55.233 | |
| CNX2I | 0.590 | |
| CNX2O | 1.386 | |
| SLP2I | 0.053 | |
| SLP2O | 0.062 | |
| CRCM3 | 6.984 | |
| CNCL3 | 54.244 | |
| CNX3I | 0.000 | |
| CNX3O | 1.063 | |
| SLP3I | 0.060 | |
| SLP3O | 0.071 | |
| RSP1I | 2.923 | |
| RSP2I | 2.884 | |
| RSP3I | 2.846 | |
| RSP1O | 3.195 | |
| RSP2O | 3.236 | |
| RSP3O | 3.272 | |
| BZSP1 | -0.130 | |
| BTSP1 | 4.565 | |
| BZ/T1 | -0.029 | |
| BZSP2 | 0.145 | |
| BTSP2 | 4.320 | |
| BZ/T2 | 0.034 | |
| ALNE | 0.288 | |
| DEN0 | 4.046 | |
| DENAV | 3.475 | |
| IP | 3.495 | |
| RKC03 | 0.000 | |
| RKC11 | 3.495 | |
| IPUNC | 3.510 | |
| PRTOT | 14.242 | |
| PRMAI | 12.419 | |
| PRDIV | 1.823 | |
| QSTAR | 2.502 | |

NEUT2 1.970E+16

# E17038

E017038 7.150 TMPW= 143.5

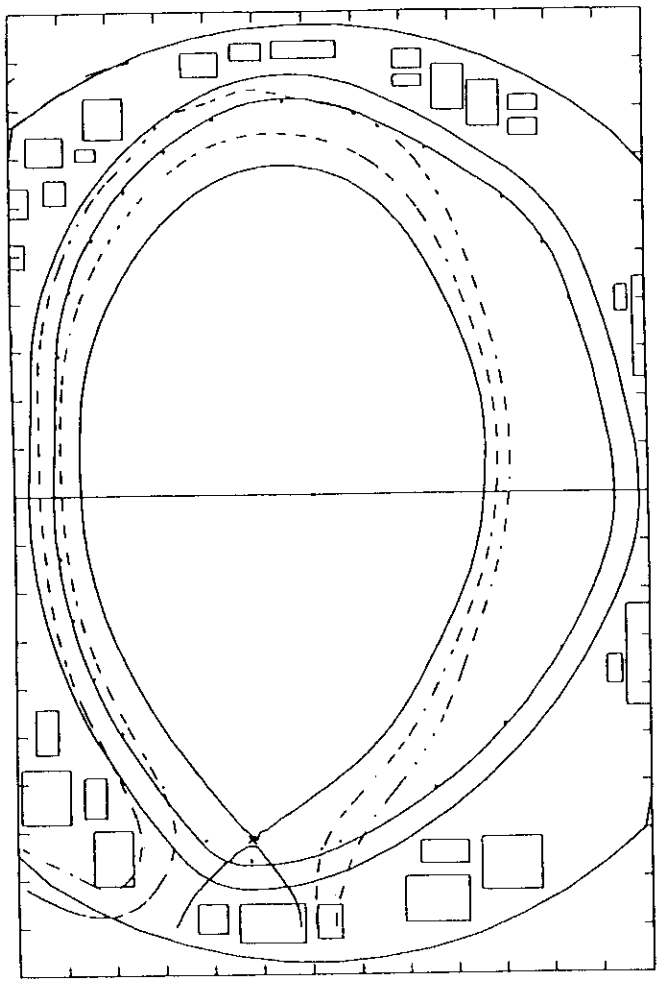

| | | |
|---|---|---|
| IP | 1.994 | MA |
| BT332 | 4.083 | T |
| RBT | 13.556 | TM |
| NEU1 | 1.547E19 | M3 |
| NEU2 | 1.900E19 | M3 |
| WDIA8 | 4.437 | MJ |
| WDA14 | 4.446 | MJ |
| WDMGC | 4.974 | MJ |
| RP | 3.200 | M |
| RJ | 3.244 | M |
| ROUT | 4.034 | M |
| RIN | 2.369 | M |
| ZP | -0.029 | M |
| ZJ | 0.091 | M |
| ZTOP | 1.366 | M |
| ZBOTM | -1.424 | M |
| A | 0.831 | M |
| AP | 1.040 | M |
| ELPAV | 1.679 | |
| TRGAV | 0.077 | |
| VOLUM | 68.076 | M3 |
| QSURF | 6.290 | |
| QEFF | 5.847 | |
| BPL0 | 1.271 | |
| BPL1 | 1.306 | |
| BETAP | 0.838 | |
| LI | 0.864 | |
| DELX | 0.087 | M |
| RSPI | 2.972 | M |
| RSEP | 3.056 | M |
| RSPO | 3.117 | M |
| ZSEP | -1.438 | M |
| ZSPI | -1.511 | M |
| ZSPO | -1.522 | M |
| IFZ | -47.121 | KA |
| IVZ | 23.977 | KA |
| IHZ | 2.994 | KA |
| IDZ | 30.043 | KA |
| IDCWZ | 0.015 | KA |
| NINDX | -1.480 | |
| NS | 0.000 | |
| BPCHI | 9.205E-02 | |
| BPCHO | 1.493E-01 | |

| | | |
|---|---|---|
| VLSM | 0.659 | V |
| PSURF | 0.534 | VS |
| PBTOT | 24.283 | MW |
| PBCO | 15.963 | MW |
| EBAVE | 82.628 | KEV |
| PBTCR | 3.957 | MW |
| PBTCO | 3.865 | MW |
| PLHT | 0.000 | MW |
| PLHC | 0.000 | MW |
| PIC | 0.000 | MW |
| PIC1 | 0.000 | MW |
| Q1 | 0.000 | PM3/S |
| Q2 | 0.000 | PM3/S |
| Q3 | 0.000 | PM3/S |
| Q4 | 0.000 | PM3/S |
| DL 0 | 53.830 | CM |
| DL 7 | 51.959 | CM |
| DL 16 | 49.126 | CM |
| DL 37 | 47.068 | CM |
| DL 47 | 46.708 | CM |
| DL 57 | 40.982 | CM |
| DL 71 | 29.011 | CM |
| DL 93 | 26.633 | CM |
| DL112 | 21.607 | CM |
| DL150 | 12.751 | CM |
| DL180 | 10.692 | CM |
| DL207 | 12.885 | CM |
| DL292 | 30.204 | CM |
| DL309 | 39.146 | CM |
| DL328 | 46.798 | CM |
| DL344 | 51.678 | CM |
| LU1 | 2.001 | M |
| LU2 | 2.316 | M |
| SL1 | 1.042 | |
| SL2 | 0.750 | |
| DRZ | -0.112 | M |
| DZZ | 0.056 | M |
| DELXZ | 0.074 | M |
| TRIGZ | 0.000 | |

| | |
|---|---|
| CRCM | 6.944 |
| CRCM1 | 7.002 |
| CNCL1 | 100.185 |
| CNX1I | 1.819 |
| CNX1O | 3.189 |
| SLP1I | 0.022 |
| SLP1O | 0.026 |
| CRCM2 | 6.966 |
| CNCL2 | 95.797 |
| CNX2I | 0.000 |
| CNX2O | 2.106 |
| SLP2I | 0.029 |
| SLP2O | 0.034 |
| CRCM3 | 6.936 |
| CNCL3 | 93.840 |
| CNX3I | 0.000 |
| CNX3O | 1.543 |
| SLP3I | 0.035 |
| SLP3O | 0.040 |
| RSP1I | 2.909 |
| RSP2I | 2.862 |
| RSP3I | 2.814 |
| RSP1O | 3.183 |
| RSP2O | 3.230 |
| RSP3O | 3.271 |
| BZSP1 | -0.056 |
| BTSP1 | 4.561 |
| BZ/T1 | -0.012 |
| BZSP2 | 0.066 |
| BTSP2 | 4.349 |
| BZ/T2 | 0.015 |
| ALNE | 0.343 |
| DEN0 | 2.372 |
| DENAV | 1.987 |
| IP | 1.994 |
| RKC03 | 0.000 |
| RKC11 | 1.994 |
| IPUNC | 2.011 |
| PRTOT | 11.660 |
| PRMAI | 4.859 |
| PRDIV | 6.801 |
| QSTAR | 4.413 |

NEUT2 1.084E+16

95-07-17 16:09:53
VER.9.0IP-RKC3,11

| | |
|---|---|
| T-PROB FITTING - | 1 |
| N-PROB FITTING - | 0 |
| FLUX FITTING - | 1 |
| NO. OF FILAMENT - | 6 |

NORM-SIGM
T= 4.113E-03
P= 4.736E-04
N= 8.734E-02
HIGH ELONG.

# E17298

E017298 5.710 TMPW= 262.7

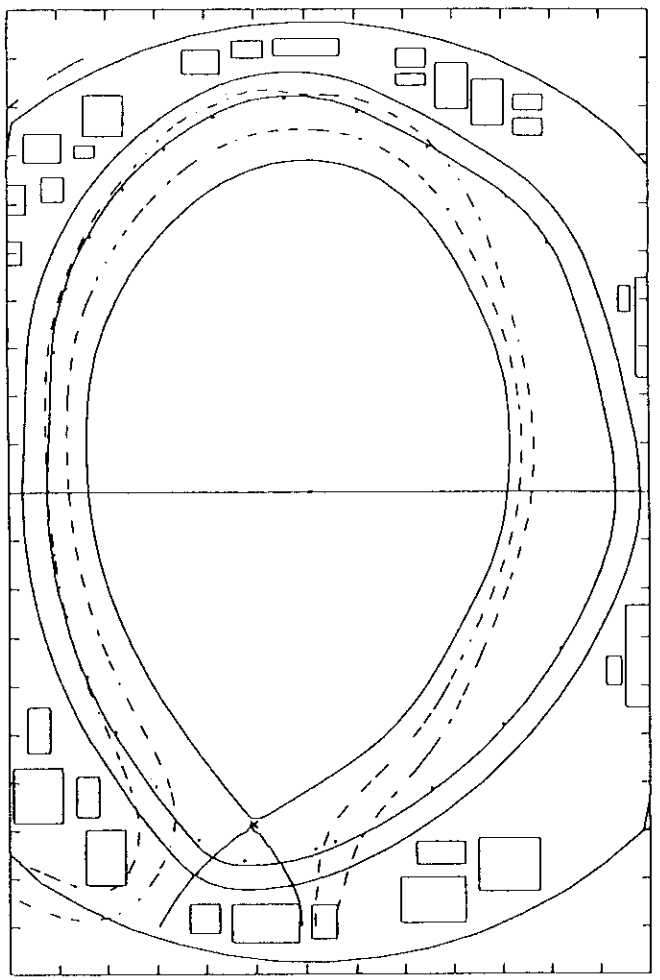

| | | |
|---|---|---|
| IP | 1.493 | MA |
| BT332 | 2.526 | T |
| RBT | 8.386 | TM |
| NEU1 | 0.841E19 | M3 |
| NEU2 | 1.321E19 | M3 |
| WDIA8 | 2.838 | MJ |
| WDA14 | 2.903 | MJ |
| WDMGC | 3.027 | MJ |
| RP | 3.275 | M |
| RJ | 3.330 | M |
| ROUT | 4.133 | M |
| RIN | 2.418 | M |
| ZP | 0.013 | M |
| ZJ | 0.139 | M |
| ZTOP | 1.379 | M |
| ZBOTM | -1.353 | M |
| A | 0.856 | M |
| AP | 1.045 | M |
| ELPAV | 1.596 | |
| TRGAV | 0.092 | |
| VOLUM | 70.359 | M3 |
| QSURF | 4.920 | |
| QEFF | 4.464 | |
| BPL0 | 1.388 | |
| BPL1 | 1.405 | |
| BETAP | 0.919 | |
| LI | 0.939 | |
| DELX | 0.148 | M |
| RSPI | 2.939 | M |
| RSEP | 3.091 | M |
| RSPO | 3.182 | M |
| ZSEP | -1.375 | M |
| ZSPI | -1.497 | M |
| ZSPO | -1.514 | M |
| IFZ | -35.530 | KA |
| IVZ | 17.594 | KA |
| IHZ | 2.136 | KA |
| IDZ | 30.020 | KA |
| IDCWZ | 0.013 | KA |
| NINDX | -1.510 | |
| NS | 0.000 | |
| BPCHI | 1.137E-01 | |
| BPCHO | 1.882E-01 | |

| | | |
|---|---|---|
| VLSM | 0.583 | V |
| PSURF | 0.365 | VS |
| PBTOT | 22.789 | MW |
| PBCO | 13.659 | MW |
| EBAVE | 89.660 | KEV |
| PBTCR | 0.000 | MW |
| PBTCO | 0.000 | MW |
| PLHT | 0.000 | MW |
| PLHC | 0.000 | MW |
| PIC | 0.000 | MW |
| PIC1 | 0.000 | MW |
| Q1 | 0.000 | PM3/S |
| Q2 | 0.000 | PM3/S |
| Q3 | 0.000 | PM3/S |
| Q4 | 0.000 | PM3/S |
| DL 0 | 44.047 | CM |
| DL 7 | 42.027 | CM |
| DL 16 | 39.058 | CM |
| DL 37 | 36.572 | CM |
| DL 47 | 36.460 | CM |
| DL 57 | 31.481 | CM |
| DL 71 | 21.708 | CM |
| DL 93 | 25.719 | CM |
| DL112 | 24.645 | CM |
| DL150 | 16.760 | CM |
| DL180 | 16.115 | CM |
| DL207 | 19.867 | CM |
| DL292 | 29.178 | CM |
| DL309 | 34.699 | CM |
| DL328 | 40.418 | CM |
| DL344 | 43.299 | CM |
| LU1 | 1.795 | M |
| LU2 | 2.389 | M |
| SL1 | 1.062 | |
| SL2 | 0.857 | |
| DRZ | -0.038 | M |
| DZZ | 0.105 | M |
| DELXZ | 0.124 | M |
| TRIGZ | 0.000 | |

| | |
|---|---|
| CRCM | 6.917 |
| CRCM1 | 7.104 |
| CNCL1 | 84.951 |
| CNX1I | 3.165 |
| CNX1O | 4.179 |
| SLP1I | 0.033 |
| SLP1O | 0.041 |
| CRCM2 | 7.069 |
| CNCL2 | 80.713 |
| CNX2I | 1.624 |
| CNX2O | 3.033 |
| SLP2I | 0.038 |
| SLP2O | 0.048 |
| CRCM3 | 7.052 |
| CNCL3 | 79.368 |
| CNX3I | 0.547 |
| CNX3O | 2.421 |
| SLP3I | 0.044 |
| SLP3O | 0.051 |
| RSP1I | 2.899 |
| RSP2I | 2.866 |
| RSP3I | 2.834 |
| RSP1O | 3.227 |
| RSP2O | 3.266 |
| RSP3O | 3.303 |
| BZSP1 | -0.076 |
| BTSP1 | 2.854 |
| BZ/T1 | -0.027 |
| BZSP2 | 0.089 |
| BTSP2 | 2.635 |
| BZ/T2 | 0.034 |
| ALNE | 0.441 |
| DEN0 | 1.688 |
| DENAV | 1.357 |
| IP | 1.493 |
| RKC03 | 0.000 |
| RKC11 | 1.493 |
| IPUNC | 1.493 |
| PRTOT | 8.474 |
| PRMAI | 6.640 |
| PRDIV | 1.834 |
| QSTAR | 3.441 |

NEUT2 5.080E+15

95-07-17 22:07:49
VER.9.0IP=RKC3,11

| | |
|---|---|
| T-PROB FITTING = | 1 |
| N-PROB FITTING = | 0 |
| FLUX FITTING = | 1 |
| NO. OF FILAMENT = | 6 |

NORM-SIGM
T= 4.052E-03
P= 3.366E-04
N= 8.975E-03
HIGH ELONG.